Combustion Fronts in a Porous Medium with Two Layers

J. C. Da Mota[1] and S. Schecter[2]

We study a model for the lateral propagation of a combustion front through a porous medium with two parallel layers having different properties. The reaction involves oxygen and a solid fuel. In each layer, the model consists of a nonlinear reaction–diffusion–convection system, derived from balance equations and Darcy's law. Under an incompressibility assumption, we obtain a simple model whose variables are temperature and unburned fuel concentration in each layer. The model includes heat transfer between the layers. We find a family of traveling wave solutions, depending on the heat transfer coefficient and other system parameters, that connect a burned state behind the combustion front to an unburned state ahead of it. These traveling waves are *strong*: they correspond to connecting orbits of a system of five ordinary differential equations that lie in the unstable manifold of a hyperbolic saddle and the stable manifold of a nonhyperbolic equilibrium. We argue that for physically relevant initial conditions, traveling waves that correspond to connecting orbits that approach the nonhyperbolic equilibrium along its center direction do not occur. When the heat transfer coefficient is small, we prove that strong traveling waves exist for a small range of system parameters, near parameter values where the two layers individually admit strong traveling waves with the same speed. When the heat transfer coefficient is large, we prove that strong traveling waves exist for a very large range of parameters. For small heat transfer, combustion typically does not occur simultaneously in the two layers; for large heat transfer, it does. The proofs use geometric singular perturbation theory. We give a numerical method to solve the nonlinear

[1]Instituto de Matemática e Estatística, Universidade Federal de Goiás, Caixa Postal 131, Campus II, 74001-970 Goiânia, GO, Brazil. E-mail: jesus@mat.ufg.br
[2]Department of Mathematics, North Carolina State University, Raleigh, NC 27695. E-mail: schecter@math.ncsu.edu

problem, and we present numerical simulations that indicate that the traveling waves we have found are in fact the dominant feature of solutions.

1. INTRODUCTION

Combustion fronts in porous media have been studied by many authors during the last few decades. In particular, for combustion processes in oil recovery, models and results of numerical simulations have been presented. One of the first models of combustion in a petroleum reservoir was formulated by Gottfried [12]. The model consists of a system of six partial differential equations describing the flow of oil, water, and gas through the porous medium, together with a chemical reaction between oxygen and oil. Numerical simulations exhibit all of the main thermal and hydrodynamic features of in situ combustion known from the laboratory, including propagation of the combustion zone, formation of a steam plateau, and formation of water and oil banks. Crookston and Culham [5] presented a general model for thermal recovery processes, as well as associated numerical procedures. In addition to the aspects of combustion processes modeled by Gottfried, they included such aspects as coke formation and oxidation.

These models are nonlinear reaction–diffusion–convection systems derived from the principle of conservation. In vector form in one space dimension, they have the form

$$H(U)_t + F(U)_x = (B(U)U_x)_x + G(U), \quad 0 < x < l, \ t > 0, \qquad (1.1)$$

where l is the length of the porous medium and U is the vector of unknown quantities, such as temperature and densities. The first and second terms in (1.1) represent, respectively, accumulation and transport by convection of these quantities; the function G represents source terms due to chemical reactions and heat loss; and the term $(B(U)U_x)_x$ represents diffusion of heat, mass, etc.

The combustion process is described by the solution of the system (1.1), with suitable initial and boundary conditions. A rigorous analysis of this solution is difficult, because the functions H, F, and G are in general nonlinear, and the number of equations and parameters in a complete model is large.

In the more recent engineering literature, several authors have given detailed analyses of aspects of combustion in porous media. In this literature, combustion fronts are assumed to exist, and jump conditions across them are derived by integration. For example, Schult et al. [20] investigated smolder combustion when gas is forced into pores in a solid reactant. Using asymptotic methods, they identify two different wave structures: a reaction-leading wave and a reaction-trailing wave. They occur when the incoming oxygen concentration is sufficiently high or low, respectively. Akkutlu and Yortsos [1] used a similar approach to study in situ combustion for oil recovery. They focus on the effects of heat loss to the surrounding rock formation. Using a jump condition across the reaction front, they derived an analytical expression relating injection velocity and temperature of the combustion front. When the injection velocity exceeds a threshold value, multiple front temperatures can occur.

Some complementary recent work identifies combustion fronts with traveling waves, and proves their existence using geometric methods. Da Mota et al. [6, 7] used this approach to study combustion fronts in a two-phase (oil and oxygen) model. Combustion fronts were identified with traveling waves connecting an unburned state ahead of the front to a burned state behind it. Schecter and Marchesin [18, 19] added heat loss to the surrounding rock formation to this model. Using geometric singular perturbation theory, they showed that for small heat loss, the combustion front is the lead part of a traveling pulse, while the trailing part of the pulse is a slow cooling process.

In all this work the porous medium consists of a single layer. However, the porous media where crude oil is found contain different layers, characterized by different porosity, density, thermal conductivity, etc.

In this paper, we study a model for combustion of oxygen and a solid fuel such as coke in a porous medium with two layers. In each layer, the model is a simplification of those considered by Gottfried and Crookston. It includes balance of energy, fuel mass, oxygen mass, and total gas mass, as well as Darcy's law, a chemical reaction rate, and heat conduction in the flow direction. The model also includes heat transfer between the layers.

We consider only the incompressible case, in which the gas density is taken to be an average value not depending on temperature or pressure. In this case, the model reduces to a system of four nonlinear partial differential equations governing temperature and unburned fuel concentration in each layer.

For this simplified system, we study traveling wave solutions that connect a completely burned state behind the reaction front to an unburned state ahead of it. The unburned state is assumed to be at the background temperature of the porous medium, which is taken to be the ignition

temperature. Such traveling waves correspond to connecting orbits in a system of five ordinary differential equations (ODEs) that lie in the unstable manifold of a hyperbolic saddle and the center-stable manifold of a nonhyperbolic equilibrium. They occur for a range of wave speeds. In combustion problems, zero eigenvalues commonly occur at equilibria corresponding to unburned states because of the form of Arrhenius's law.

When the connecting orbit lies in the stable manifold of the nonhyperbolic equilibrium, it and the corresponding traveling wave are called *strong*. In our model, strong traveling waves typically occur only for isolated values of the wave speed. We argue that for physically relevant initial conditions, only strong traveling waves occur. We prove the existence of a family of strong traveling waves parameterized by the heat transfer coefficient and other system parameters.

The proofs use normally hyperbolic invariant manifolds and geometric singular perturbation theory, which are frequently used in the study of traveling waves (for background in these areas, see [9, 13], and for an application to combustion, see [11]). We mention in particular the paper of Bose [2], which studies a "two-layer" model: nerve-conduction along two parallel nerve fibers. The issue in [2] is different, however: the two fibers have exactly the same physical properties, and the question is which traveling waves persist when there is small coupling between them. The present two-layer model can perhaps serve as a prototype for other two-layer traveling-wave problems in which the layers have different properties; the features we find should occur in other situations.

The importance of the strong combustion waves that we find theoretically is demonstrated by numerical simulations of the system, in which it is observed that any injection gas temperature above a threshold value produces a solution that includes one of these combustion waves. The wave selected depends only on the heat transfer coefficient and other system parameters, not the injection temperature.

We now preview the remainder of the paper.

In Section 2, we describe the full model. Under an incompressibility assumption, we obtain the simplified system that we shall study.

In Section 3, we derive the ODEs that govern traveling waves. We then introduce a new variable that represents cumulative heat transfer between the two layers. This permits us to integrate some of the equations. We show that finding traveling waves is equivalent to finding orbits connecting certain equilibria in a system of five ODEs, in which the wave speed is a parameter.

If there is no heat transfer between the layers, the two-layer problem reduces to two decoupled one-layer problems. Such one-layer problems are studied in Section 4. A system of two ODEs, in which the wave speed is

a parameter, governs the existence of traveling waves. We prove that for a range of wave speeds, there exist connections from a saddle to a non-hyperbolic equilibrium. For one value of the wave speed, the connection is strong. The other connections arrive at the nonhyperbolic equilibrium along its center direction.

Numerical results, along with theoretical considerations, indicate that only the strong connection corresponds to traveling combustion fronts in solutions of the PDE for physically important initial conditions. A similar fact was observed in [7]. We therefore, focus our attention on strong connections.

In Section 5, we begin the analysis of the 5-dimensional ODE system. We identify equilibria and determine their eigenvalues.

We study separately, in Sections 6 and 7, respectively, the cases of large and small heat transfer between the two layers. These two cases are accessible to a rigorous geometric singular perturbation treatment.

When the heat transfer coefficient is large, we show that the two-layer system is essentially a one-layer system with two types of fuel. We show that for all values of the system parameters, strong traveling waves exist for sufficiently large heat transfer coefficient. The temperatures in the two layers stay close throughout the wave.

When the heat transfer coefficient is small, we show that strong traveling waves exist for a small range of system parameters, near the codimension-one manifold M of parameter values for which the two layers individually admit strong traveling waves with the same speed. The waves of the two-layer system have a fast-changing part and a slowly changing part. In the fast part, where combustion occurs, the solution jumps quickly from the unburned state to an intermediate state with (typically) different combustion front temperatures in each layer. Within the fast jump, the solution typically jumps first in one layer, then the other. In other words, combustion does not occur simultaneously in the two layers as it does for large heat transfer coefficient. In the slow part of the wave, behind the combustion zone, the temperature of the two layers slowly equilibrates due to heat transfer between the layers.

For fixed small heat transfer coefficient, as the system parameters move away from M, the separation between the combustion fronts in the two layers increases. Of course, if the gap is large enough, such a traveling wave will not be observed in a reservoir of finite length.

A Melnikov integral calculation needed in Section 7 is posponed to Section 8.

In Section 9, we present numerical simulations of the PDE that show the development of the traveling wave that we have found theoretically. The features of the traveling wave that we have identified are clearly seen.

We also present ODE simulations that show the traveling wave directly as a connecting orbit. Details of the numerical method that we use for the PDE, including a discussion of convergence, are deferred to a separate paper.

Our results are consistent with the possibility that traveling waves exist for all values of the system parameters and heat transfer coefficient. It may be possible to prove this using Conley index techniques. Nevertheless, the features of the wave that we find by the geometric singular perturbation analysis are clearly of importance.

2. MODEL

We consider a horizontal one-dimensional porous medium consisting of two parallel layers, each with an initially available concentration of a solid fuel such as coke. The space variable is x, $0 < x < l$, and time is t, $t > 0$. A schematic of the medium geometry is shown in Figure 1. The chemical reaction in each layer takes the simple form

[solid reactant] + [gaseous reactant] $\rightarrow$ [gaseous product] + [heat].

$$(2.1)$$
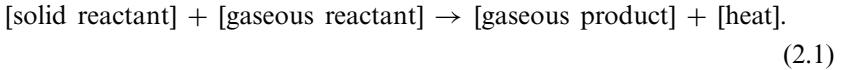
To formulate balance equations, we assume that gas, rock matrix, and fuel are locally and at all times in thermal equilibrium in each layer. Hence, only one temperature is used for the energy balance in each layer. Porosity in each layer is assumed constant and independent of the the fuel concentration. Heat loss to the surrounding rock formation is neglected. However, a reaction rate, longitudinal heat conduction, and heat transfer between the two layers are taken into account.

Subscripts g, r, and c refer to oxygen, rock, and coke, respectively, and the subscript s refers to an entire layer. Subscripts 1 and 2 designate the two layers.

In the ith layer, the state variables depending on (x, t) are temperature T_{s_i}, fuel concentration η_{c_i}, oxygen mass fraction in the gas phase Y_i, seepage velocity v_{g_i}, and pressure p_{s_i}.
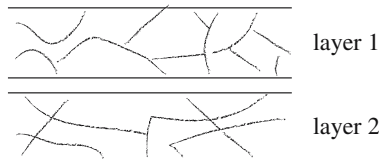

Figure 1. Porous medium.

The other relevant quantities in the ith layer are gas density ρ_{g_i}, given by a layer-independent equation of state $\rho_{g_i} = \rho_g(T_{s_i}, p_{s_i})$; rock density ρ_{r_i}; porosity ϕ_i; thermal conductivity λ_{s_i}; heat capacity of gas at constant pressure c_{g_i}; specific heat of rock c_{r_i}; rate of coke consumption in the chemical reaction r_i; mass–weighted stoichiometric coefficients for oxygen and gas m_i and m_{g_i}, respectively (see [1]). The quantity m_{g_i} may be positive, negative, or zero, depending on whether the amount of gas produced by the reaction is more than, less than, or equal to the amount of gas consumed by it. Quantities assumed to be the same for both layers are: specific heat of coke c_c; heat of reaction Q_c; flow resistance appearing in Darcy's law K_s, which is directly proportional to rock permeability and inversely proportional to gas viscosity. Finally, the coefficient of heat transfer between the two layers is denoted by Q_l.

The following equations are assumed to hold in the ith layer, $i = 1, 2$:
Balance of energy

$$\frac{\partial}{\partial t}\left(\phi_i \rho_{g_i} c_{g_i} T_{s_i} + (1 - \phi_i)\rho_{r_i} c_{r_i} T_{s_i} + \eta_{c_i} c_c T_{s_i}\right)$$
$$= -\frac{\partial}{\partial x}\left(\rho_{g_i} c_{g_i} v_{g_i} T_{s_i}\right) + Q_c r_i - Q_l(T_{s_i} - T_{s_{3-i}}) + \lambda_{s_i}\frac{\partial^2 T_{s_i}}{\partial x^2}. \quad (2.2)$$

Balance of fuel mass

$$\frac{\partial \eta_{c_i}}{\partial t} = -r_i. \quad (2.3)$$

Balance of oxygen mass

$$\frac{\partial}{\partial t}(\phi_i \rho_{g_i} Y_i) + \frac{\partial}{\partial x}(\rho_{g_i} v_{g_i} Y_i) = -m_i r_i. \quad (2.4)$$

Balance of total gas mass

$$\frac{\partial}{\partial t}(\phi_i \rho_{g_i}) + \frac{\partial}{\partial x}(\rho_{g_i} v_{g_i}) = m_{g_i} r_i. \quad (2.5)$$

Darcy's law

$$v_{g_i} = -K_s\frac{\partial p_{s_i}}{\partial x}. \quad (2.6)$$

The rate of coke consumption in the chemical reaction, in each layer, is assumed to be given by a version of Arrhenius's law:

$$r_i = A_{c_i}(Y_i p_{s_i})^\alpha \eta_{c_i} e^{-E/RT_{s_i}} \text{ if } T_{s_i} > 0, \text{ and } r_i = 0 \text{ if } T_{s_i} \leqslant 0, \quad (2.7)$$

where A_{c_i} is the Arrhenius constant, E the activation energy, α the order of the gaseous reaction rate, and R is the gas constant. E and α are

assumed to be the same for both layers. Temperature has been shifted so that the ignition temperature is $T_{s_i} = 0$.

We introduce dimensionless variables for space and time,

$$\tilde{x} = \frac{x}{x^*}, \qquad \tilde{t} = \frac{t}{t^*}, \tag{2.8}$$

where x^* and t^* are reference values for space and time, respectively. A dimensionless seepage velocity in the ith layer is given by

$$v_i = \frac{t^* v_{g_i}}{x^*}. \tag{2.9}$$

We also introduce dimensionless variables for temperature, fuel concentration, pressure, and gas density in the ith layer,

$$T_i = \frac{T_{s_i}}{T^*}, \quad p_i = \frac{p_{s_i}}{p^*}, \quad \rho_i = \frac{\rho_{g_i}}{\rho_g^*} \quad \text{and} \quad \eta_i = \frac{\eta_{c_i}}{\eta_{c_i}^o}, \tag{2.10}$$

where T^*, p^*, and ρ_g^* are reference values for temperature, pressure, and gas density, respectively; and $\eta_{c_i}^o$ is the initial fuel concentration in the ith layer. Thus η_i is the fraction of coke remaining in the ith layer, $0 \leqslant \eta_i \leqslant 1$. The reference gas density ρ_g^* is obtained from the reference temperature and pressure using the state equation.

With these dimensionless variables, and after dropping the tildes from x and t to simplify the notation, the systems (2.2)–(2.6) becomes

$$\frac{\partial}{\partial t}\left(\left(\phi_i \rho_g^* \rho_i c_{g_i} + (1-\phi_i)\rho_{r_i} c_{r_i} + \eta_{c_i}^o c_c \eta_i\right) T_i\right) = -\frac{\partial}{\partial x}\left(\rho_g^* \rho_i c_{g_i} v_i T_i\right)$$
$$+\frac{t^* \eta_{c_i}^o A_{c_i} Q_c (p^*)^\alpha}{T^*} h(T_i, \eta_i, Y_i, p_i) - t^* Q_l (T_i - T_{3-i}) + \frac{t^* \lambda_{s_i}}{(x^*)^2} \frac{\partial^2 T_i}{\partial x^2}, \quad i = 1, 2, \tag{2.11}$$

$$\frac{\partial \eta_i}{\partial t} = -t^* A_{c_i} (p^*)^\alpha h(T_i, \eta_i, Y_i, p_i), \quad i = 1, 2, \tag{2.12}$$

$$\frac{\partial}{\partial t}(\phi_i \rho_g^* \rho_i Y_i) + \frac{\partial}{\partial x}(\rho_g^* \rho_i v_i Y_i) = -t^* m_i \rho_{c_i}^o A_{c_i} (p^*)^\alpha h(T_i, \eta_i, Y_i, p_i), \quad i = 1, 2, \tag{2.13}$$

$$\frac{\partial}{\partial t}(\phi_i \rho_g^* \rho_i) + \frac{\partial}{\partial x}(\rho_g^* \rho_i v_i) = t^* m_{g_i} \rho_{c_i}^o A_{c_i} (p^*)^\alpha h(T_i, \eta_i, Y_i, p_i), \quad i = 1, 2, \tag{2.14}$$

$$v_i = -\frac{t^* p^* K_s}{(x^*)^2} \frac{\partial p_i}{\partial x}, \quad i = 1, 2, \tag{2.15}$$

where h is the nondimensional function

$$h(T, \eta, Y, p) = (Yp)^\alpha \eta\, e^{-E/RT^*T} \quad \text{if } T > 0, \quad \text{and} \quad h(T, \eta, Y, p) = 0$$
$$\text{if } T \leqslant 0. \tag{2.16}$$

Finally, we divide (2.11) by the mean value $\bar{\rho_r}\bar{c_r} = \frac{1}{2}\big((1 - \phi_1)\rho_{r_1} c_{r_1} + (1 - \phi_2)\rho_{r_2} c_{r_2}\big)$, and (2.13) and (2.14) by the reference gas density $\rho_g^* = \rho_g(T^*, p^*)$. The reason for dividing Eq. (2.11) by the given constant is that all parameters in the resulting equation vary in a range convenient for numerical computation. We obtain the system

$$\frac{\partial}{\partial t}\big((a_i + b_i \eta_i)T_i\big) + \frac{\partial}{\partial x}(c_i v_i T_i) = d_i\, h(T_i, \eta_i, Y_i, p_i) - q(T_i - T_{3-i}) + \lambda_i \frac{\partial^2 T_i}{\partial x^2},$$
$$i = 1, 2, \tag{2.17}$$

$$\frac{\partial \eta_i}{\partial t} = -A_i\, h(T_i, \eta_i, Y_i, p_i), \quad i = 1, 2, \tag{2.18}$$

$$\frac{\partial}{\partial t}(\phi_i \rho_i Y_i) + \frac{\partial}{\partial x}(\rho_i v_i Y_i) = -B_i\, h(T_i, \eta_i, Y_i, p_i), \quad i = 1, 2, \tag{2.19}$$

$$\frac{\partial}{\partial t}(\phi_i \rho_i) + \frac{\partial}{\partial x}(\rho_i v_i) = D_i\, h(T_i, \eta_i, Y_i, p_i), \quad i = 1, 2, \tag{2.20}$$

$$v_i = -K \frac{\partial p_i}{\partial x}, \quad i = 1, 2, \tag{2.21}$$

$0 < x < l$, $t > 0$, where

$$a_i = \frac{\phi_i \rho_g^* \rho_i c_{g_i} + (1 - \phi_i)\rho_{r_i} c_{r_i}}{\bar{\rho_r}\bar{c_r}}, \quad b_i = \frac{\eta_{c_i}^o c_c}{\bar{\rho_r}\bar{c_r}}, \quad c_i = \frac{\rho_g^* \rho_i c_{g_i}}{\bar{\rho_r}\bar{c_r}}, \tag{2.22}$$

$$A_i = t^* A_{c_i}(p^*)^\alpha, \quad d_i = \frac{A_i \eta_{c_i}^o Q_c}{T^* \bar{\rho_r}\bar{c_r}}, \quad \lambda_i = \frac{t^* \lambda_{s_i}}{(x^*)^2 \bar{\rho_r}\bar{c_r}}, \quad q = \frac{t^* Q_l}{\bar{\rho_r}\bar{c_r}}, \tag{2.23}$$

$$B_i = \frac{m_i A_i \eta_{c_i}^o}{\rho_g^*}, \quad D_i = \frac{m_{g_i} A_i \eta_{c_i}^o}{\rho_g^*}, \quad \text{and} \quad K = \frac{t^* p^* K_s}{(x^*)^2}. \tag{2.24}$$

The quantities defined in (2.22)–(2.24) depend on the physical properties of the two layers, and they are all nonnegative, except D_i, which, depending on the stoichiometric coefficient m_{g_i}, may be positive, negative, or zero.

From now on, we shall assume that the fluids are incompressible, and we shall neglect volume and pressure changes due to the chemical reaction. These assumptions simplify our equations and isolate the main temperature and fuel consumption effects. Thus, for $i = 1, 2$, ρ_i is constant, independent of temperature and pressure; $m_{g_i} = 0$; and therefore, $D_i = 0$.

We are interested in the physical situation in which gas is injected into the porous medium at $x = 0$, all the coke burns, and a reaction front propagates to the right. Since $D_i = 0$, from (2.20) we have $\frac{\partial v_i}{\partial x} = 0$, so v_i depends on time only. One can relate it to boundary conditions at the injection end. For simplicity we assume it to be constant. Also, from (2.21), we see that p_i can be easily calculated using the injection pressure.

Equations (2.17) and (2.18) are coupled with Eq. (2.19) only by the factor $(Y_i p_i)^\alpha$ in the function h. For simplicity we take this factor to be a known constant average value.

With these simplifications, from Eqs. (2.17) and (2.18) we obtain the following system modeling temperature and fuel concentration. To simplify the notation we rename the temperature and the fuel concentration in the two layers $u = T_1$, $y = \eta_1$, $v = T_2$, and $z = \eta_2$.

$$\frac{\partial}{\partial t}\left((a_1 + b_1 y)u\right) + \frac{\partial}{\partial x}(c_1 u) = d_1 f(u, y) - q(u - v) + \lambda_1 \frac{\partial^2 u}{\partial x^2}, \quad (2.25)$$

$$\frac{\partial y}{\partial t} = -A_1 f(u, y), \quad (2.26)$$

$$\frac{\partial}{\partial t}\left((a_2 + b_2 z)v\right) + \frac{\partial}{\partial x}(c_2 v) = d_2 f(v, z) - q(v - u) + \lambda_2 \frac{\partial^2 v}{\partial x^2}, \quad (2.27)$$

$$\frac{\partial z}{\partial t} = -A_2 f(v, z), \quad (2.28)$$

$0 < x < l$, $t > 0$. Here f is defined by

$$f(w, \eta) = \eta e^{-E/RT^* w} \quad \text{if } w > 0, \quad \text{and} \quad f(w, \eta) = 0 \quad \text{if } w \leqslant 0. \quad (2.29)$$

All parameters are those defined in (2.22) and (2.23), except A_1 and A_2, now defined by

$$A_i = t^* A_{c_i} (p^* Y_i p_i)^\alpha, \quad i = 1, 2. \quad (2.30)$$

3. TRAVELING WAVE SYSTEM

We shall look for combustion fronts as traveling wave solutions of the system (2.25)–(2.28). We therefore replace the spatial domain $0 < x < l$ by $\mathbb{R}$.
Following [19] we define

$$\Omega = \left\{ h : \mathbb{R} \to \mathbb{R} : h \in C^1, \lim_{\xi \to \pm\infty} h(\xi) \text{ exists, and } \lim_{\xi \to \pm\infty} \frac{dh}{d\xi} = 0 \right\}.$$

Let $\Omega^n = \Omega \times \cdots \times \Omega$ (n times).
Given $X = (h_1, \ldots, h_n)$ in Ω^n, let

$$X^\pm = \lim_{\xi \to \pm\infty} X(\xi) = \lim_{\xi \to \pm\infty} \left(h_1(\xi), \ldots, h_n(\xi) \right) = (h_1^\pm, \ldots, h_n^\pm). \qquad (3.1)$$

Definition 3.1. A traveling wave of the systems (2.25)–(2.28) with speed σ, connecting a state $W_0 = (u_0, y_0, v_0, z_0)$ on the left to a state $W_1 = (u_1, y_1, v_1, z_1)$ on the right, is a solution $W(\xi) = \left(u(\xi), y(\xi), v(\xi), z(\xi) \right)$ in Ω^4, with $\xi = x - \sigma t$, satisfying the boundary conditions

$$W^- = W_0 \qquad \text{and} \qquad W^+ = W_1. \qquad (3.2)$$

We are interested in traveling waves that connect a burned state (one with $y = z = 0$) on the left to an unburned state (one with $y = z = 1$) on the right. We recall (see the paragraph that includes Eq. (2.7)) that the temperature scale has been shifted so that, in accordance with Arrhenius's law, the ignition temperature is $u = 0$. We shall assume that the background reservoir temperature is also $u = 0$. In other words, combustion does not occur at the background reservoir temperature; it begins at any higher temperature. In the simulations reported in Section 9, the traveling waves that develop have the temperature at the unburned state equal to the background reservoir temperature. This seems to be the case whenever the initial temperature profile is everywhere greater than or equal to the background reservoir temperature. Since this is the physically relevant case, we consider only traveling waves with unburned states that are at the background reservoir temperature in both layers, i.e., $u = v = 0$. The following proposition gives a necessary and sufficient condition for the existence of such a traveling wave of (2.25)–(2.28).

Proposition 3.2. *If $W(\xi) = \left(u(\xi), y(\xi), v(\xi), z(\xi) \right)$ is a traveling wave with speed σ of the system (2.25)–(2.28) connecting $W_L = (u_L, 0, v_L, 0)$ on the left to $W_R = (0, 1, 0, 1)$ on the right, then there exist a function w in Ω*

and a number w_L such that $X(\xi) = \big(u(\xi), y(\xi), v(\xi), z(\xi), w(\xi)\big)$ is a solution of the system

$$\dot{u} = \frac{1}{\lambda_1}\left(-\sigma\left(a_1 u + b_1 uy + \frac{d_1}{A_1}y - \frac{d_1}{A_1}\right) + c_1 u - w\right), \tag{3.3}$$

$$\dot{y} = \frac{A_1}{\sigma}f(u, y), \tag{3.4}$$

$$\dot{v} = \frac{1}{\lambda_2}\left(-\sigma\left(a_2 v + b_2 vz + \frac{d_2}{A_2}z - \frac{d_2}{A_2}\right) + c_2 v + w\right), \tag{3.5}$$

$$\dot{z} = \frac{A_2}{\sigma}f(v, z), \tag{3.6}$$

$$\dot{w} = q(v - u) \tag{3.7}$$

satisfying

$$X^- = X_L = (u_L, 0, v_L, 0, w_L) \quad and \quad X^+ = X_R = (0, 1, 0, 1, 0). \tag{3.8}$$

Conversely, if $X(\xi) = \big(u(\xi), y(\xi), v(\xi), z(\xi), w(\xi)\big)$ is a solution in Ω^5 of (3.3)–(3.7) satisfying (3.8), then $W(\xi) = \big(u(\xi), y(\xi), v(\xi), z(\xi)\big)$ is a traveling wave with speed σ of the systems (2.25)–(2.28) connecting W_L to W_R.

Proof. Suppose $W(\xi) = \big(u(\xi), y(\xi), v(\xi), z(\xi)\big)$, $\xi = x - \sigma t$, is a traveling wave of (2.25)–(2.28) connecting W_L to W_R. Substituting $W(\xi)$ in (2.25)–(2.28), we have

$$-\sigma\frac{d}{d\xi}\big((a_1 + b_1 y)u\big) + \frac{d}{d\xi}(c_1 u) = d_1 f(u, y) - q(u - v) + \lambda_1 \frac{d^2 u}{d\xi^2}, \tag{3.9}$$

$$\sigma\frac{dy}{d\xi} = A_1 f(u, y), \tag{3.10}$$

$$-\sigma\frac{d}{d\xi}\big((a_2 + b_2 z)v\big) + \frac{d}{d\xi}(d_2 v) = d_2 f(v, z) + q(u - v) + \lambda_2 \frac{d^2 v}{d\xi^2}, \tag{3.11}$$

$$\sigma\frac{dz}{d\xi} = A_2 f(v, z). \tag{3.12}$$

Integrating Eqs. (3.10) and (3.12) from ξ to ∞, and using the boundary conditions $y(\infty) = z(\infty) = 1$, we obtain

$$\sigma - \sigma y = A_1 \int_\xi^\infty f(u, y)\,d\tilde{\xi} \quad and \quad \sigma - \sigma z = A_2 \int_\xi^\infty f(v, z)\,d\tilde{\xi}. \tag{3.13}$$

Therefore, the integrals converge, and

$$\int_\xi^\infty f(u, y)\,d\tilde{\xi} = \frac{\sigma}{A_1}(1 - y) \quad and \quad \int_\xi^\infty f(v, z)\,d\tilde{\xi} = \frac{\sigma}{A_2}(1 - z). \tag{3.14}$$

Integrating (3.9) and (3.11) from ξ to ∞, and using the boundary conditions $u(\infty) = v(\infty) = \dot{u}(\infty) = \dot{v}(\infty) = 0$, we obtain

$$\lambda_1 \dot{u} = -\sigma(a_1 + b_1 y)u + c_1 u + d_1 \int_\xi^\infty f(u, y)\, d\tilde{\xi} - \int_\xi^\infty q(u - v)\, d\tilde{\xi}, \quad (3.15)$$

$$\lambda_2 \dot{v} = -\sigma(a_2 + b_2 z)v + c_2 v + d_2 \int_\xi^\infty f(v, z)d\tilde{\xi} - \int_\xi^\infty q(v - u)\, d\tilde{\xi}. \quad (3.16)$$

Since the integrals in (3.14) converge, so do the remaining integrals in (3.15) and (3.16). Then the system (3.3)–(3.7) is obtained by defining

$$w = \int_\xi^\infty q(u - v)\, d\tilde{\xi} \qquad (3.17)$$

and substituting (3.14) and (3.17) into (3.15) and (3.16).

We still must show that $w(-\infty)$ is finite, $w(\infty) = 0$, and $\dot{w}(\pm\infty) = 0$. From (3.17), we see immediately that $w(\infty) = 0$. The fact that $w(-\infty) = \int_{-\infty}^\infty q(u - v)\, d\tilde{\xi}$ is finite follows from integrating (3.15) or (3.16) from $\xi = -\infty$ to $\xi = \infty$ and using (3.14) and the boundary conditions at $\xi = -\infty$. From (3.17), we see that $\dot{w} = q(u - v)$. For $q = 0$ we have immediately that $\dot{w} = 0$. For $q > 0$ we see from the boundary conditions that $\dot{w}(-\infty) = u_L - v_L$ and $\dot{w}(\infty) = 0 - 0 = 0$. The fact that $\int_{-\infty}^\infty q(u - v)\, d\tilde{\xi}$ converges implies that $u_L = v_L$.

Conversely, suppose that $X(\xi) = \big(u(\xi), y(\xi), v(\xi), z(\xi), w(\xi)\big)$, $\xi = x - \sigma t$, is a solution in Ω^5 of the systems (3.3)–(3.7) satisfying the boundary condition (3.8). Differentiating (3.3) and (3.5) with respect ξ, and using (3.4), (3.6), and (3.7), we easily complete the proof. $\qquad\square$

Where convenient, we shall write (3.3)–(3.7) as follows:

$$\dot{U} = G(U, w, \sigma, \Pi), \qquad (3.18)$$
$$\dot{V} = H(V, w, \sigma, \Pi), \qquad (3.19)$$
$$\dot{w} = q(v - u) \qquad (3.20)$$

with $U = (u, y)$, $V = (v, z)$, $G = (G_1, G_2)$, $H = (H_1, H_2)$, and Π the vector of system parameters (including the parameters that appear in the definition of f in (2.29)). We have $X = (U, V, w)$. We shall also write the systems (3.18)–(3.20) as follows:

$$\dot{X} = F(X, \sigma, \Pi, q) = \big(G(U, w, \sigma, \Pi), H(V, w, \sigma, \Pi), q(v - u)\big). \quad (3.21)$$

All system parameters are assumed to be positive.

4. COMBUSTION FRONTS IN ONE LAYER

If $q=0$, the PDEs (2.25) and (2.26), and (2.27) and (2.28), which govern layers 1 and 2, respectively, decouple. Traveling waves of (2.25) and (2.26) that connect an unburned state to a burned state satisfy (3.18) with $w=0$, i.e., $\dot{U}=\hat{G}(U,\sigma,\Pi)=G(U,0,\sigma,\Pi)$, or

$$\dot{u} = \frac{1}{\lambda_1}\left(-\sigma\left(a_1 u+b_1 uy+\frac{d_1}{A_1}y-\frac{d_1}{A_1}\right)+c_1 u\right), \tag{4.1}$$

$$\dot{y} = \frac{A_1}{\sigma}f(u,y). \tag{4.2}$$

In this section, we study this system. Our notation will often suppress the dependence on Π, but will always show the dependence on σ.

Physically relevant solutions must have $0\leqslant y\leqslant 1$. However, in order to have a clear picture of solutions in this region, it is convenient to consider all solutions in the upper half plane $y\geqslant 0$.

We note that in the open first quadrant $u>0$, $y>0$, we have $\dot{y}>0$. When $y=0$, $\dot{y}=0$, so the u-axis is invariant. Also, for $u\leqslant 0$, $\dot{y}=0$, so the vector field is horizontal (see Figure 2).

We assume

(A1) $\sigma>\frac{c_1}{a_1}$.

In particular, σ is positive. Note that $\frac{c_1}{a_1}$ is small because the rock density is much larger than the gas density. From (A1), for $y\geqslant 0$, $\dot{u}$ is positive, 0, or negative according to whether (u,y) is below, on, or above the curve

$$u=\frac{\sigma d_1(1-y)}{A_1(\sigma a_1+\sigma b_1 y-c_1)}. \tag{4.3}$$

This curve crosses the u-axis at

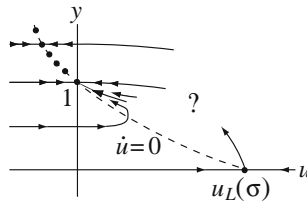$$u_L(\sigma)=\frac{\sigma d_1}{A_1(\sigma a_1-c_1)}>0. \tag{4.4}$$

Figure 2. Phase portrait of (4.1) and (4.2).

Thus the the equilibria of the systems (4.1) and (4.2) in the region $y \geqslant 0$ are $(u_L(\sigma), 0)$ and the curve given by (4.3) with $y \geqslant 1$. This curve lies in the nonphysical region $y > 1$ except for the point $(0, 1)$.

We therefore look for solutions in Ω^2 of (4.1) and (4.2) that satisfy the boundary conditions

$$U^- = U_L(\sigma) = (u_L(\sigma), 0) \quad \text{and} \quad U^+ = U_R = (0, 1). \tag{4.5}$$

Solutions of (4.1) and (4.2), (4.5) correspond to traveling waves with speed σ in a one-layer system that connect the burned state $(u_L(\sigma), 0)$ on the left to the unburned state $(0, 1)$ on the right.

Note that for $\sigma < \frac{c_1}{a_1}$ we have $u_L(\sigma) < 0$. Since the vector field is horizontal there, traveling waves with left state $(u_L(\sigma), 0)$ cannot exist.

We have

$$D_U \hat{G}(U_L(\sigma), \sigma) = \begin{pmatrix} a_{11} & a_{12} \\ 0 & a_{22} \end{pmatrix} \quad \text{and} \quad D_U \hat{G}(U_R, \sigma) = \begin{pmatrix} b_{11} & b_{12} \\ 0 & 0 \end{pmatrix}, \tag{4.6}$$

where

$$a_{11} = -\frac{\sigma a_1 - c_1}{\lambda_1}, \quad a_{12} = -\frac{\sigma}{\lambda_1}\left(b_1 u_L(\sigma) + \frac{d_1}{A_1}\right), \quad a_{22} = \frac{A_1}{\sigma} f_y(u_L(\sigma), 0),$$

$$b_{11} = -\frac{\sigma a_1 + \sigma b_1 - c_1}{\lambda_1}, \quad \text{and} \quad b_{12} = -\frac{\sigma d_1}{\lambda_1 A_1}. \tag{4.7}$$

Using (A1), we see that the eigenvalues at $U_L(\sigma)$ are $a_{11} < 0$ and $a_{22} > 0$. Corresponding eigenvectors are $(1, 0)$ and $(a_{12}, a_{22} - a_{11})$. Thus $U_L(\sigma)$ is a saddle, and its stable manifold is the u-axis. The vector $(a_{12}, a_{22} - a_{11})$, which is tangent to the unstable manifold of $U_L(\sigma)$, has first component negative and second component positive.

The eigenvalues at U_R are $b_{11} < 0$ and 0, with corresponding eigenvectors $(1, 0)$ and $(-b_{12}, b_{11})$, which has first component positive and second component negative. The latter is tangent to the center manifold of U_R, which consists of the curve of equilibria in $u \leqslant 0$ and an orbit in $u > 0$. Since $\dot{y} > 0$ when $u > 0$, motion on this orbit is toward U_R. The stable manifold of U_R (and of every equilibrium in $u \leqslant 0$) has horizontal tangent. From center manifold theory [3], points in $u > 0$ that are near U_R and below its stable manifold lie in orbits that approach U_R tangent to its 0 eigenvector. Points in $u > 0$ that are near U_R and above its stable manifold lie in the stable manifold of an equilibrium in $u < 0$ (see Figure 2).

Definition 4.1. A connecting orbit of an ODE from a hyperbolic equilibrium U_L to a nonhyperbolic equilibrium U_R is called *strong* if it lies in the stable manifold of U_R. If the connecting orbit corresponds to a traveling wave of a PDE, the traveling wave is also called strong.

Theorem 4.2. *There is a number σ^*, with $\frac{c_1}{a_1} < \sigma^* < \infty$, such that the system (4.1) and (4.2) has a connecting orbit from $U_L(\sigma)$ to U_R if and only if $\sigma^* \leqslant \sigma < \infty$. The connecting orbit is strong if and only if $\sigma = \sigma^*$.*

Proof. We shall show that, in the region $u > 0$, the stable manifold of U_R lies below the unstable manifold of $U_L(\sigma)$ for small σ and above it for large σ. Hence there is an intermediate value $\sigma = \sigma^*$ for which a strong connection exists. We shall use a Melnikov integral calculation to show that σ^* is unique.

To study large σ, in (4.1) and (4.2) we let $\sigma = \frac{1}{\epsilon}$ and $\xi = \epsilon\eta$. Using $'$ to denote derivative with respect to η, we obtain

$$u' = \frac{1}{\lambda_1}\left(-\left(a_1 u + b_1 uy + \frac{d_1}{A_1}y - \frac{d_1}{A_1}\right) + \epsilon c_1 u\right), \tag{4.8}$$

$$y' = \epsilon^2 A_1 f(u, y). \tag{4.9}$$

For $\epsilon = 0$, the system (4.8) and (4.9) has the curve of equilibria $u = \frac{d_1(1-y)}{A_1(a_1+b_1 y)}$, which includes a segment in the first quadrant that joins $\left(\frac{d_1}{a_1 A_1}, 0\right)$ to $(0, 1)$. This segment of equilibria is normally hyperbolic (the nonzero eigenvalue is negative). Therefore, for small positive ϵ it persists as an invariant curve. Near the u-axis this curve coincides with the unstable manifold of $U_L(\frac{1}{\epsilon})$, and near the y-axis it approaches $(0, 1)$ tangent to its center direction. It therefore contains a connecting orbit of (4.8) and (4.9) from $U_L(\frac{1}{\epsilon})$ to U_R that is not strong. Thus for large σ there is a connecting orbit of (4.1) and (4.2) from $U_L(\sigma)$ to U_R that is not strong. Because the stable manifold of U_R is approximately horizontal, we see that for large $\sigma > 0$, in the region $u > 0$, the stable manifold of $(0, 1)$ lies above the unstable manifold of $U_L(\sigma)$.

To study small $\sigma > \frac{c_1}{a_1}$, in (4.1) and (4.2) we let $\sigma = \frac{c_1}{a_1} + \tau$. Since $u_L(\sigma) \to \infty$ as $\sigma \to \frac{c_1}{a_1}$, we also make the change of variables $u = \frac{1}{s}$. We obtain the following system for $s > 0$ (corresponding to $u > 0$):

$$s' = \frac{s}{\lambda_1}\left(\left(\frac{c_1}{a_1} + \tau\right)\left(a_1 + b_1 y + \frac{d_1}{A_1}(y-1)s\right) - c_1\right), \tag{4.10}$$

$$y' = \frac{A_1 a_1}{c_1 + a_1 \tau} y e^{-\frac{E}{R}s}. \tag{4.11}$$

Equilibria of (4.1) and (4.2) with $u \leqslant 0$ are not visible in this system; in particular, U_R has moved to $s = \infty$.

Setting $\tau = 0$ in (4.10) and (4.11), we obtain

$$s' = \frac{c_1}{a_1\lambda_1} s\left(b_1 y + \frac{d_1}{A_1}(y-1)s\right), \tag{4.12}$$

$$y' = \frac{A_1 a_1}{c_1} y e^{-\frac{E}{R}s}. \tag{4.13}$$

There is a unique equilibrium at $(s, y) = (0, 0)$, with eigenvalues $\frac{A_1 a_1}{c_1} > 0$ and 0. The unstable manifold is the y-axis; a center manifold is the s-axis, on which $s' = -\frac{c_1 d_1}{A_1 a_1 \lambda_1} s^2$.

For $\tau > 0$ this equilibrium perturbs to a repeller at $(0, 0)$ and a saddle at $(s, 0)$ with $s = \frac{A_1 a_1^2 \tau}{d_1(a_1\tau + c_1)}$. The saddle is just $U_L(\frac{c_1}{a_1} + \tau)$. Given any compact part of the y-axis, for small $\tau > 0$ the unstable manifold of the saddle is near it. Returning to (u, y)-coordinates, we see that the last fact implies that for small $\sigma > \frac{c_1}{a_1}$, in the region $u > 0$, the stable manifold of U_R lies below the unstable manifold of $U_L(\sigma)$, so there is no connection.

Since, in the region $u > 0$, the stable manifold of U_R lies below the unstable manifold of $U_L(\sigma)$ for small σ and above it for large σ, there is an intermediate value $\sigma = \sigma^*$ for which a strong connection exists.

We can define a separation function between $W^s(U_R)$ and $W^u(U_L(\sigma))$ that is negative (respectively, positive) when the former is below (respectively, above) the latter. For later use we denote the separation function $\hat{S}_1(\sigma, \Pi)$, indicating the dependence on Π and that it is the separation function for layer 1.

At a point (σ^*, Π^*) where the separation is 0 (i.e., where there is a strong connection), let the connecting solution be $U^*(\xi) = (u^*(\xi), y^*(\xi))$, and let

$$\hat{\psi}_1(\xi) = \exp\left(-\int_0^\xi \mathrm{div}\ \hat{G}(U^*(\tau), \sigma^*, \Pi^*)\, d\tau\right)(-\dot{y}^*(\xi)\ \dot{u}^*(\xi)), \tag{4.14}$$

a row vector. Then for r equal to σ or any component of Π, we have the well-known Melnikov integral formula: up to a positive multiple,

$$\frac{\partial \hat{S}_1}{\partial r}(\sigma^*, \Pi^*) = \int_{-\infty}^{\infty} \hat{\psi}_1(\xi)\frac{\partial \hat{G}}{\partial r}(U^*(\xi), \sigma^*, \Pi^*)\, d\xi. \tag{4.15}$$

We remark that Melnikov integrals can have an additional term when there is a nonhyperbolic equilibrium present, if the equilibrium changes as parameters vary [4, 16]. Here, however, the nonhyperbolic equilibrium is always $(0, 1)$.

To compute $\frac{\partial \hat{S}_1}{\partial \sigma}(\sigma^*, \Pi^*)$ using (4.15), we note that along any solution $U(\xi) = \big(u(\xi), y(\xi)\big)$,

$$
\big(-\dot{y}(\xi) \ \dot{u}(\xi)\big) \frac{\partial \hat{G}}{\partial \sigma}\big(U(\xi), \sigma, \Pi\big) = \ \dot{y} \cdot \frac{1}{\lambda_1}\left(a_1 u + b_1 u y + \frac{d_1}{A_1} y - \frac{d_1}{A_1}\right)
$$
$$
-\dot{u} \cdot \frac{A_1}{\sigma^2} f(u, y). \tag{4.16}
$$

From the phase portrait (Figure 2), $\dot{u} < 0$ along any connection from U_L to U_R, so, using (4.3),

$$
u > \frac{\sigma d_1 (1 - y)}{A_1(\sigma a_1 + \sigma b_1 y - c_1)} > \frac{\sigma d_1 (1 - y)}{A_1(\sigma a_1 + \sigma b_1 y)} = \frac{d_1 (1 - y)}{A_1(a_1 + b_1 y)}.
$$

Therefore in (4.16), the quantity $a_1 u + b_1 u y + \frac{d_1}{A_1} y - \frac{d_1}{A_1}$ must be positive along any connection. Also, $\dot{y} > 0$ in the first quadrant, where any connection lies. It follows that (4.16) is positive along any strong connection, so $\frac{\partial \hat{S}_1}{\partial \sigma}(\sigma^*, \Pi^*)$ is positive. Therefore, at any strong connection the separation function goes from negative to positive as σ increases. It follows that the value of σ at which a strong connection exists is unique. $\qquad\square$

Numerical simulations of the one-layer system (2.25) and (2.26) with $q = 0$ indicate that only combustion fronts corresponding to strong connections of (4.1) and (4.2) actually form. In particular, different injection temperatures at the left give rise to traveling waves with a speed σ^* that is independent of the injection temperature. Largely for this reason, we reject the other connections as nonphysical.

There are at least two additional reasons to reject the other connections:

(1) If $\big(u^*(\xi), y^*(\xi)\big)$ is a strong connection, then for any finite ξ_0, $\int_{\xi_0}^{\infty} u^*(\xi) \, d\xi$ is finite, because $u^*(\xi)$ approaches 0 exponentially. Thus the total heat ahead of the combustion front is finite. This conclusion does not hold for connections that are not strong. However, in simulations, the initial temperature profile $u(x, 0)$ typically has $\int_{x_0}^{\infty} u(x, 0) \, dx$ finite for any finite x_0; in fact, the initial temperature is typically equal to the background reservoir temperature, which we have taken to be 0, to the right of some point. For such initial conditions, which are the physically relevant ones, one can wonder how there could develop an infinite amount of heat ahead of the combustion front.

(2) In other combustion contexts, the addition to the equations of perturbation terms such as heat loss to the rock formation causes the zero eigenvalues at unburned states to become positive, thus eliminating connections that are not strong. (However, the burned states remain

equilibria, even though they are nonhyperbolic before perturbation.) (See [18]).

5. EQUILIBRIA OF THE TWO-LAYER TRAVELING WAVE SYSTEM

In the remainder of the paper, we study the two-layer traveling wave systems (3.18)–(3.20). Analagously to (A1), we assume throughout the rest of the paper:

(B1) $\sigma > \max\left(\frac{c_1}{a_1}, \frac{c_2}{a_2}\right)$.

An easy consequence of (B1) is

$$\sigma > \frac{c_1 + c_2}{a_1 + a_2}. \tag{5.1}$$

In this section, we investigate the equilibria of (3.18)–(3.20). We consider the physically relevant region $0 \leqslant y \leqslant 1$, $0 \leqslant z \leqslant 1$. For $q = 0$ and given (σ, Π), the equilibria of (3.3)–(3.7) in this region include: (1) a unique point with $u = v = 0$, $X_R = (0, 1, 0, 1, 0)$; and (2) a curve of points with $y = z = 0$,

$$X_L(w, \sigma, \Pi) = \big(u_L(w, \sigma, \Pi), 0, v_L(w, \sigma, \Pi), 0, w\big),$$

$$u_L(w, \sigma, \Pi) = \frac{\sigma d_1 - A_1 w}{A_1(\sigma a_1 - c_1)}, \quad v_L(w, \sigma, \Pi) = \frac{\sigma d_2 + A_2 w}{A_2(\sigma a_2 - c_2)}. \tag{5.2}$$

There are two additional curves of equilibria in the physical region, one with $y = v = 0$, and one with $u = z = 0$, that we shall not consider here.

For $q > 0$ and given (σ, Π), there are just two equilibria in the physical region: (1) X_R and (2) $X_L(\sigma, \Pi) = X_L\big(w_L(\sigma, \Pi), \sigma, \Pi\big)$, where the function $w_L(\sigma, \Pi)$ is obtained by solving the equation

$$v - u = v_L(w, \sigma, \Pi) - u_L(w, \sigma, \Pi) = \left(\frac{\sigma d_2}{A_2(\sigma a_2 - c_2)} - \frac{\sigma d_1}{A_1(\sigma a_1 - c_1)}\right)$$
$$+ \left(\frac{1}{\sigma a_1 - c_1} + \frac{1}{\sigma a_2 - c_2}\right) w = 0 \tag{5.3}$$

for w. Then $X_L(\sigma, \Pi) = \big(u_L(\sigma, \Pi), 0, v_L(\sigma, \Pi), 0, w_L(\sigma, \Pi)\big)$ with

$$u_L(\sigma, \Pi) = v_L(\sigma, \Pi) = \sigma \frac{d_1 A_2 + d_2 A_1}{A_1 A_2 \big(\sigma(a_1 + a_2) - (c_1 + c_2)\big)},$$

$$w_L(\sigma, \Pi) = \sigma \frac{d_1 A_2(\sigma a_2 - c_2) - d_2 A_1(\sigma a_1 - c_1)}{A_1 A_2 \big(\sigma(a_1 + a_2) - (c_1 + c_2)\big)}. \tag{5.4}$$

From (B1) and (5.1), the denominators in (5.3) and (5.4) are positive. Note that $X_L(\sigma, \Pi)$ is an equilibrium for any q.

Proposition 5.1. (1) *For $q=0$, those equilibria $X_L(w, \sigma, \Pi)$ of (3.18)–(3.20) for which $u_L(w, \sigma, \Pi) > 0$ and $v_L(w, \sigma, \Pi) > 0$ have two negative eigenvalues, one zero eigenvalue, and two positive eigenvalues. The equilibria X_R have two negative eigenvalues and three zero eigenvalues.*

(2) *For $q > 0$, the equilibria $X_L(\sigma, \Pi)$ of (3.18)–(3.20) all have $u_L(\sigma, \Pi) = v_L(\sigma, \Pi) > 0$. They have two eigenvalues with negative real part and three positive eigenvalues. The equilibria X_R have two negative eigenvalues, two zero eigenvalues, and one positive eigenvalue.*

Proof. We have $u_L(\sigma, \Pi) = v_L(\sigma, \Pi) > 0$ by (5.4). The Jacobian matrix of (3.18)–(3.20) is

$$
\begin{aligned}
&J = D_X F(X, \sigma, \Pi, q) \\
&= \begin{pmatrix}
-\frac{1}{\lambda_1}\left(\sigma(a_1 + b_1 y) - c_1\right) & -\frac{\sigma}{\lambda_1}\left(b_1 u + \frac{d_1}{A_1}\right) & 0 & 0 & -\frac{1}{\lambda_1} \\
\frac{A_1}{\sigma} f_u(u, y) & \frac{A_1}{\sigma} f_y(u, y) & 0 & 0 & 0 \\
0 & 0 & -\frac{1}{\lambda_2}\left(\sigma(a_2 + b_2 z) - c_2\right) & -\frac{\sigma}{\lambda_2}\left(b_2 v + \frac{d_2}{A_2}\right) & \frac{1}{\lambda_2} \\
0 & 0 & \frac{A_2}{\sigma} f_v(v, z) & \frac{A_2}{\sigma} f_z(v, z) & 0 \\
-q & 0 & q & 0 & 0
\end{pmatrix}.
\end{aligned}
$$

$$(5.5)$$

At a point with $y = z = 0$, (5.5) becomes

$$
J = D_X F(u, 0, v, 0, \sigma, \Pi, q) = \begin{pmatrix}
a_{11} & a_{12} & 0 & 0 & -\frac{1}{\lambda_1} \\
0 & a_{22} & 0 & 0 & 0 \\
0 & 0 & a_{33} & a_{34} & \frac{1}{\lambda_2} \\
0 & 0 & 0 & a_{44} & 0 \\
-q & 0 & q & 0 & 0
\end{pmatrix}
\qquad (5.6)
$$

with

$$
a_{11} = -\frac{1}{\lambda_1}(\sigma a_1 - c_1), \quad a_{12} = -\frac{\sigma}{\lambda_1}\left(b_1 u + \frac{d_1}{A_1}\right), \quad a_{22} = \frac{A_1}{\sigma} f_y(u, 0),
$$

$$
a_{33} = -\frac{1}{\lambda_2}(\sigma a_2 - c_2), \quad a_{34} = -\frac{\sigma}{\lambda_2}\left(b_2 v + \frac{d_2}{A_2}\right), \quad a_{44} = \frac{A_2}{\sigma} f_z(v, 0).
$$

We have

$$
\det(\Lambda I - J) = (\Lambda - a_{22})(\Lambda - a_{44})\left(\Lambda^3 - (a_{11} + a_{33})\Lambda^2 \right.
$$

$$
\left. + \left(a_{11} a_{33} - \frac{q}{\lambda_1} - \frac{q}{\lambda_2}\right)\Lambda + \frac{q a_{11}}{\lambda_2} + \frac{q a_{33}}{\lambda_1}\right).
$$

Thus, two eigenvalues of (5.6) are a_{22} and a_{44}; they are positive if u and v are positive. For $q = 0$, the other three eigenvalues are $a_{11} < 0$, $a_{33} < 0$, and 0. For $q > 0$, the other three eigenvalues have sum $a_{11} + a_{33} < 0$ and product $-q\left(\frac{a_{11}}{\lambda_2} + \frac{a_{33}}{\lambda_1}\right) > 0$. Hence two have negative real part and one is positive.

At X_R, (5.5) becomes

$$J = D_X F(X_R, \sigma, \Pi, q) = \begin{pmatrix} b_{11} & b_{12} & 0 & 0 & -\frac{1}{\lambda_1} \\ 0 & 0 & 0 & 0 & 0 \\ 0 & 0 & b_{33} & b_{34} & \frac{1}{\lambda_2} \\ 0 & 0 & 0 & 0 & 0 \\ -q & 0 & q & 0 & 0 \end{pmatrix} \tag{5.7}$$

with $b_{11} = -\frac{1}{\lambda_1}(\sigma a_1 + \sigma b_1 - c_1)$, $b_{12} = -\frac{\sigma d_1}{\lambda_1 A_1}$, $b_{33} = -\frac{1}{\lambda_2}(\sigma a_2 + \sigma b_2 - c_2)$,

and $b_{34} = -\frac{\sigma d_2}{\lambda_2 A_2}$. We have

$$\det(\Lambda I - J) = \Lambda^2 \left(\Lambda^3 - (b_{11} + b_{33})\Lambda^2 + \left(b_{11}b_{33} - \frac{q}{\lambda_1} - \frac{q}{\lambda_2}\right)\Lambda + \frac{qb_{11}}{\lambda_2} + \frac{qb_{33}}{\lambda_1}\right).$$

Thus, two eigenvalues of (5.7) are 0. For $q = 0$, the other three eigenvalues are $b_{11} < 0$, $b_{33} < 0$, and 0. For $q > 0$, two have negative real part and one is positive. □

Since for $q > 0$ the unstable manifold of $X_L(\sigma, \Pi)$ has dimension 3 and the center-stable manifold of X_R has dimension 4, connections are expected to exist for a range of σ. However, since the stable manifold of X_R has dimension 2, strong connections are expected to exist only for isolated values of σ. As in the one-layer case, numerical simulations indicate that only combustion fronts corresponding to strong connections actually form. Therefore, in the remainder of the paper we focus on the existence of strong connections from $X_L(\sigma, \Pi)$ to X_R.

6. COMBUSTION FRONTS IN TWO LAYERS FOR LARGE q

In this section, we show that if the heat transfer coefficient q is sufficiently large, then strong traveling waves of the two-layer system exist. We fix the values of the system parameters, and generally suppress dependence on the system parameters in the notation.

Theorem 6.1. *For any fixed values Π of the system parameters, there exists a number q^* such that for all $q > q^*$, there is a wave speed $\sigma^*(q)$ such that the traveling wave systems (3.18)–(3.20) with $\sigma = \sigma^*(q)$ has a strong*

connection from $X_L(\sigma^*, \Pi)$ to X_R. Moreover, $u(\xi)$ and $v(\xi)$ are close along the connection.

The proof also shows that for any compact subset K of system parameter space, a single value of q^* can be chosen. However, we do not know if the wave speed $\sigma^*(q)$ is unique.

The remainder of this section is devoted to proving Theorem 6.1. In the course of the proof, we shall see that for large q, the system is close one that describes combustion in one layer with two types of fuel (see (6.18)–(6.20)).

The plan of the proof is as follows. To study the traveling wave systems (3.3)–(3.7) for large q, we make the change of variables

$$q = \frac{1}{\epsilon^2}, \quad w = \frac{\omega}{\epsilon}, \quad \xi = \epsilon\eta. \tag{6.1}$$

In the new system, we identify a 3-dimensional normally hyperbolic invariant manifold $S(\sigma, \Pi, \epsilon)$ on which $u \approx v$. After restricting to $S(\sigma, \Pi, \epsilon)$, the connections we seek correspond to connecting orbits in a 3-dimensional system from a hyperbolic equilibrium with 2-dimensional unstable manifold to a nonhyperbolic equilibrium with 1-dimensional stable manifold. This system, to lowest order, describes combustion in one layer with two types of fuel; the layer has physical properties intermediate between those of the original layers. As in the proof of Theorem 4.2, we show that for small (respectively, large) σ, the stable manifold lies below (respectively, above) the unstable manifold. Therefore, they meet for some intermediate σ. Actually, we describe the relative positions of these manifolds not in these terms, but in terms of where the stable manifold leaves a certain box.

Let

$$h(u, y, \sigma, \Pi) = \frac{1}{\lambda_1}\left(-\sigma\left(a_1 u + b_1 u y + \frac{d_1}{A_1}y - \frac{d_1}{A_1}\right) + c_1 u\right),$$

$$k(v, z, \sigma, \Pi) = \frac{1}{\lambda_2}\left(-\sigma\left(a_2 v + b_2 v z + \frac{d_2}{A_2}z - \frac{d_2}{A_2}\right) + c_2 v\right).$$

Making the change of coordinates (6.1) and using $'$ to denote $\frac{d}{d\eta}$, we obtain the system

$$u' = \epsilon h(u, y, \sigma, \Pi) - \frac{\omega}{\lambda_1}, \tag{6.2}$$

$$y' = \epsilon\frac{A_1}{\sigma}f(u, y), \tag{6.3}$$

$$v' = \epsilon k(v, z, \sigma, \Pi) + \frac{\omega}{\lambda_2}, \tag{6.4}$$

$$z' = \epsilon \frac{A_2}{\sigma} f(v, z), \tag{6.5}$$

$$\omega' = v - u. \tag{6.6}$$

We set $\epsilon = 0$ in (6.2)–(6.6) and obtain the linear system

$$u' = -\frac{\omega}{\lambda_1}, \tag{6.7}$$

$$y' = 0, \tag{6.8}$$

$$v' = \frac{\omega}{\lambda_2}, \tag{6.9}$$

$$z' = 0, \tag{6.10}$$

$$\omega' = v - u. \tag{6.11}$$

There is a 3-dimensional plane of equilibria $S = \{(u, y, v, z, \omega) : v = u$ and $\omega = 0\}$. The eigenvalues of the systems (6.7)–(6.11) are 0, 0, 0, $\pm\left(\frac{1}{\lambda_1} + \frac{1}{\lambda_2}\right)^{\frac{1}{2}}$, so S is a normally hyperbolic.

For small $\epsilon > 0$, any compact part of S perturbs to a normally hyperbolic invariant manifold $S(\sigma, \Pi, \epsilon)$, given by equations of the form

$$v = A(u, y, z, \sigma, \Pi, \epsilon) = u + \epsilon a(u, y, z, \sigma, \Pi) + O(\epsilon^2), \tag{6.12}$$

$$\omega = B(u, y, z, \sigma, \Pi, \epsilon) = \epsilon b(u, y, z, \sigma, \Pi) + O(\epsilon^2). \tag{6.13}$$

Since each $S(\sigma, \Pi, \epsilon)$ is invariant, we can differentiate (6.12) and (6.13) with respect to η and obtain

$$v' = u' + \epsilon \left(\frac{\partial a}{\partial u} u' + \frac{\partial a}{\partial y} y' + \frac{\partial a}{\partial z} z' \right) + O(\epsilon^2), \tag{6.14}$$

$$\omega' = \epsilon \left(\frac{\partial b}{\partial u} u' + \frac{\partial b}{\partial y} y' + \frac{\partial b}{\partial z} z' \right) + O(\epsilon^2). \tag{6.15}$$

Substituting (6.2)–(6.6) and (6.12) and (6.13) into (6.14) and (6.15), we obtain

$$\epsilon k(u + O(\epsilon), z, \sigma, \Pi) + \frac{1}{\lambda_2}(\epsilon b + O(\epsilon^2)) = \epsilon h(u, y, \sigma, \Pi)$$

$$-\frac{1}{\lambda_1}(\epsilon b + O(\epsilon^2)) + \epsilon \left(\frac{\partial a}{\partial u} O(\epsilon) + \frac{\partial a}{\partial y} O(\epsilon) + \frac{\partial a}{\partial z} O(\epsilon) + O(\epsilon) \right), \tag{6.16}$$

$$\epsilon(a + O(\epsilon)) = \epsilon \left(\frac{\partial b}{\partial u} O(\epsilon) + \frac{\partial b}{\partial y} O(\epsilon) + \frac{\partial b}{\partial z} O(\epsilon) + O(\epsilon) \right). \tag{6.17}$$

From the order ϵ terms in (6.16) and (6.17), we obtain

$$a = 0 \quad \text{and } b = \frac{\lambda_1 \lambda_2}{\lambda_1 + \lambda_2} \big(h(u, y, \sigma, \Pi) - k(u, z, \sigma, \Pi) \big).$$

We obtain the differential equation on $S(\sigma, \Pi, \epsilon)$ to order ϵ, in the variables (u, y, z), by substituting (6.12) and (6.13) into (6.2) and (6.3) and (6.5). In the fast time $\xi = \epsilon \eta$ we obtain

$$\dot{u} = \frac{1}{\lambda_1 + \lambda_2} \big(\lambda_1 h(u, y, \sigma, \Pi) + \lambda_2 k(u, z, \sigma, \Pi) \big), \tag{6.18}$$

$$\dot{y} = \frac{A_1}{\sigma} f(u, y), \tag{6.19}$$

$$\dot{z} = \frac{A_2}{\sigma} f(u, z) \tag{6.20}$$

plus terms of order ϵ.

We first study (6.18)–(6.20), i.e., we set $\epsilon = 0$. This system describes one layer with two types of fuel and intermediate physical properties. From (6.18) we have

$$\left(\frac{\partial \dot{u}}{\partial u}, \frac{\partial \dot{u}}{\partial y}, \frac{\partial \dot{u}}{\partial z} \right) = -\frac{\lambda_1 \lambda_2}{\lambda_1 + \lambda_2} \left(\sigma(a_1 + a_2 + b_1 y + b_2 z) - (c_1 + c_2), \sigma \frac{d_1}{A_1}, \sigma \frac{d_2}{A_2} \right). \tag{6.21}$$

For $y \geqslant 0$ and $z \geqslant 0$, (5.1) implies that all three components of (6.21) are negative. We have $\dot{u} = 0$ if and only if

$$u = \frac{\sigma \left(\frac{d_1}{A_1}(1 - y) + \frac{d_2}{A_2}(1 - z) \right)}{\sigma(a_1 + a_2 + b_1 y + b_2 z) - (c_1 + c_2)}. \tag{6.22}$$

Note that $u_L(\sigma, \Pi)$, defined by (5.4), is given by setting $y = z = 0$ in (6.22). We consider the region $R(\sigma, \Pi)$ in uyz-space defined by $0 \leqslant u \leqslant u_L(\sigma, \Pi)$, $0 \leqslant y \leqslant 1$, $0 \leqslant z \leqslant 1$. The equilibria of (6.18)–(6.20) in $R(\sigma, \Pi)$ are $(u_L(\sigma, \Pi), 0, 0)$ and $(0, 1, 1)$. The region $R(\sigma, \Pi)$, the equilibria, and the surface (6.22) are shown in Figure 3.

The equilibrium $(u_L(\sigma, \Pi), 0, 0)$ has two positive eigenvalues and one negative eigenvalue. The stable manifold is contained in the u-axis. The equilibrium $(0, 1, 1)$ has one negative eigenvalue and two zero eigenvalues. The stable manifold is tangent to the vector $(1, 0, 0)$. We are interested in connections from $(u_L(\sigma, \Pi), 0, 0)$ to $(0, 1, 1)$ that arrive in the stable manifold of the latter.

Notice that $\dot{y} > 0$ for $y > 0$ and $\dot{z} > 0$ for $z > 0$. Therefore (1) the portion of $W^s_{\text{loc}}(0, 1, 1)$ in $u > 0$ lies in $R(\sigma, \Pi)$; and (2) in backwards time,
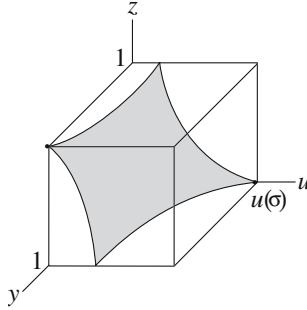
Figure 3. The surface $\dot{u} = 0$ for $\epsilon = 0$ in uyz-space; $\dot{u}$ is negative above the surface and positive below it.

$W^s(0, 1, 1)$ cannot leave $R(\sigma, \Pi)$ through its faces $y = 1$ or $z = 1$. Moreover, since the planes $y = 0$ and $z = 0$ are invariant, in backwards time $W^s(0, 1, 1)$ cannot leave $R(\sigma, \Pi)$ through them either. Therefore, in backwards time $W^s(0, 1, 1)$ either (1) leaves $R(\sigma, \Pi)$ through the interior of its face $u = 0$, (2) leaves $R(\sigma, \Pi)$ through the interior of its face $u = u_L(\sigma, \Pi)$, or (3) approaches $(u_L(\sigma, \Pi), 0, 0)$. In case 3, we have a connection from $(u_L(\sigma, \Pi), 0, 0)$ to $(0, 1, 1)$ of the desired type. Since (see Figure 3) $\dot{u} > 0$ in the interior of the face $u = 0$, and $\dot{u} < 0$ in the interior of the face $u = u_L(\sigma, \Pi)$, cases 1 and 2 each occur for an open set of σ. Hence, to show that case 3 occurs for some $\sigma > \frac{c_1 + c_2}{a_1 + a_2}$, we only need to show that cases 1 and 2 both occur for nonempty sets of σ.

To study large σ, we set $\sigma = \frac{1}{\delta}$ in (6.18)–(6.20), multiply the resulting differential equation by δ (which amounts to a rescaling of time), and obtain

$$\dot{u} = -\frac{1}{\lambda_1 + \lambda_2}\left(a_1 u + b_1 u y + \frac{d_1}{A_1}(y - 1) + \delta c_1 u + a_2 u + b_2 u z\right.$$
$$\left. + \frac{d_2}{A_2}(z - 1) + \delta c_2 v\right), \tag{6.23}$$

$$\dot{y} = \delta^2 A_1 f(u, y), \tag{6.24}$$
$$\dot{z} = \delta^2 A_2 f(u, z). \tag{6.25}$$

For $\delta = 0$, the systems (6.23)–(6.25) has an equilibrium at $(0, 1, 1)$ with two zero eigenvalues and one negative eigenvalue, and stable manifold equal to the line $y = z = 1$.

The point $(0, 1, 1)$ persists as an equilibrium for $\delta > 0$, with one-dimensional stable manifold. Let

$$\bar{u} = \frac{\frac{d_1}{A_1} + \frac{d_2}{A_2}}{a_1 + a_2}.$$

For small $\delta > 0$, the portion of the stable manifold of $(0, 1, 1)$ with $0 \leqslant u \leqslant 2\bar{u}$ is close to the line $y = z = 1$. Also, for small $\delta > 0$, the region $R(\sigma, \Pi)$ with $\sigma = \frac{1}{\delta}$ is close to the region $0 \leqslant u \leqslant \bar{u}$, $0 \leqslant y \leqslant 1$, $0 \leqslant z \leqslant 1$. It follows that for large σ, which corresponds to small δ, we are in case 2.

To study small $\sigma > \frac{c_1 + c_2}{a_1 + a_2}$, we let $\sigma = \frac{c_1 + c_2}{a_1 + a_2} + \tau$. Since $u_L(\sigma) \to \infty$ as $\sigma \to \frac{c_1 + c_2}{a_1 + a_2}$, we also make the change of variables $s = \frac{1}{u}$ for $u > 0$. We obtain, for $s > 0$,

$$\dot{s} = \frac{s}{\lambda_1 + \lambda_2}\left(\left(\frac{c_1 + c_2}{a_1 + a_2} + \tau\right)\right.$$
$$\left(a_1 + a_2 + b_1 y + b_2 z + \frac{d_1}{A_1}(y - 1)s + \frac{d_2}{A_2}(z - 1)s\right)$$
$$\left. - (c_1 + c_2)\right), \tag{6.26}$$

$$\dot{y} = A_1 \frac{a_1 + a_2}{c_1 + c_2}\left(1 - \frac{a_1 + a_2}{c_1 + c_2}\tau + O(\tau^2)\right)ye^{-\frac{E}{R}s}, \tag{6.27}$$

$$\dot{z} = A_2 \frac{a_1 + a_2}{c_1 + c_2}\left(1 - \frac{a_1 + a_2}{c_1 + c_2}\tau + O(\tau^2)\right)ze^{-\frac{E}{R}s}. \tag{6.28}$$

Setting $\tau = 0$, we have, for $s > 0$,

$$\dot{s} = \frac{c_1 + c_2}{(a_1 + a_2)(\lambda_1 + \lambda_2)}s\left(b_1 y + b_2 z + \frac{d_1}{A_1}(y - 1)s\right.$$
$$\left. + \frac{d_2}{A_2}(z - 1)s\right), \tag{6.29}$$

$$\dot{y} = A_1 \frac{a_1 + a_2}{c_1 + c_2}ye^{-\frac{E}{R}s}, \tag{6.30}$$

$$\dot{z} = A_2 \frac{a_1 + a_2}{c_1 + c_2}ze^{-\frac{E}{R}s}. \tag{6.31}$$

The equilibria $(0, 1, 1)$ of (6.18)–(6.20) here occur for $s = \infty$ and therefore are not visible. There is however an equilibrium at $(s, y, z) = (0, 0, 0)$. It has two positive eigenvalues and one 0 eigenvalue. The unstable manifold is the yz-plane; a center manifold is the s-axis, on which $\dot{s} = -\frac{c_1 + c_2}{(a_1 + a_2)(\lambda_1 + \lambda_2)}\left(\frac{d_1}{A_1} + \frac{d_2}{A_2}\right)s^2$.

For small $\tau > 0$ the equilibrium $(0, 0, 0)$ of (6.29)–(6.31) perturbs to a repeller at $(0, 0, 0)$ and a saddle at $(s, 0, 0)$ with $s = \frac{a\tau}{\frac{d_1}{A_1} + \frac{d_2}{A_2}}$. Given any compact part of the yz-plane, the unstable manifold of the latter equilibrium is near it for small $\tau > 0$.

Returning to (u, y, z)-coordinates and the system (6.18)–(6.20), we see that the last fact implies for small $\sigma > \frac{c_1 + c_2}{a_1 + a_2}$, in the region $0 \leqslant y \leqslant 1$,

$0 \leqslant z \leqslant 1$, $W^u(u_L(\sigma, \Pi), 0, 0)$ is close to the plane $u = u_L(\sigma, \Pi)$. Since in the interior of the face $u = u_L(\sigma, \Pi)$ of $R(\sigma, \Pi)$, we have $\dot{u} < 0$, points of $W^u(u_L(\sigma, \Pi), 0, 0)$ near this face lie in $R(\sigma, \Pi)$. This invariant manifold prevents cases 2 and 3, so we are in case 1.

Since we have case 1 for small σ and case 2 for large σ, we must have case 3 for some intermediate σ.

For $\epsilon > 0$, we note that there are equilibria of the system (6.2)–(6.6) at $(u_L(\sigma, \Pi), 0, u_L(\sigma, \Pi), 0, \epsilon w_L(\sigma, \Pi))$ and $(0, 1, 0, 1, 0)$. Since these equilibria must lie in $S(\sigma, \Pi, \epsilon)$, we see that for $\epsilon > 0$, the system (6.18)–(6.20), with the perturbation in ϵ included, still has equilibria at $(u_L(\sigma, \Pi), 0, 0)$ and $(0, 1, 1)$. Therefore for $\epsilon > 0$ we consider the perturbed system (6.18)–(6.20) in $R(\sigma, \Pi)$.

Recall that all three components of (6.21) are negative in $R(\sigma, \Pi)$. It follows that given $\tau_0 > 0$, for sufficiently small $\epsilon_0 > 0$, if

$$\frac{c_1 + c_2}{a_1 + a_2} + \tau_0 \leqslant \sigma \leqslant \frac{1}{\tau_0} \quad \text{and} \quad 0 \leqslant \epsilon \leqslant \epsilon_0, \tag{6.32}$$

then the surface $\dot{u} = 0$ is situated as in Figure 3.

We have $\dot{y} \geqslant 0$ and $\dot{z} \geqslant 0$ everywhere; and for (τ, ϵ) satisfying (6.32), on the face $y = 1$ (respectively, $z = 1$) of $R(\sigma, \Pi)$, $\dot{y} > 0$ (respectively, $\dot{z} > 0$) except possibly near $u = 0$. It follows that, as for $\epsilon = 0$, there are three possible cases for where $W^s(0, 1, 1)$ leaves $R(\sigma, \Pi)$, and cases 1 and 2 each occur for an open set of σ. Perturbing from the $\epsilon = 0$ situation, we easily see that case 1 occurs for small σ and case 2 for large σ, so case 3 must occur for some intermediate σ. Case 3 corresponds to a strong connections of (3.3)–(3.7) from $X_L(\sigma, \Pi)$ to X_R.

7. COMBUSTION FRONTS IN TWO LAYERS FOR SMALL q

In this section, we investigate the existence of strong traveling waves in (3.18)–(3.20) for small $q > 0$. Let P denote system parameter space. There are functions σ_1 and σ_2 defined on P such that if $\Pi \in P$ is a vector of system parameters, then for $q = 0$, in layers 1 and 2 there are strong traveling waves with speeds $\sigma_1(\Pi)$ and $\sigma_2(\Pi)$, respectively. (This follows from Section 4, where we showed that the derivative of the one-layer separation function with respect to σ is nonzero.) Let M denote the set of points in P where $\sigma_1 = \sigma_2$. A point $\Pi \in M$ is called *regular* if $D(\sigma_1 - \sigma_2)(\Pi) \neq 0$. Near any regular point of M, M is a codimension one submanifold of P. Whereas for large q we were able to investigate arbitrary vectors of system parameters, for small $q > 0$ we shall only be able to study vectors of system parameters near regular points of M.

Theorem 7.1. *Let Π^* be a regular point of M, and let $\sigma^* = \sigma_1(\Pi^*) = \sigma_2(\Pi^*)$. Then for small $q > 0$ there is an open subset U_q of P near Π^* such that for $\Pi \in U_q$, the systems (3.3)–(3.7), with vector of parameters Π, has a strong traveling wave with speed near σ^*.*

In the remainder of this section, we give the proof of this result, except for a computation that is left to Section 8.

Write $\Pi = (\tilde{\Pi}, \pi)$, where π is one of the system parameters and $\tilde{\Pi}$ is the rest. The system parameter π is chosen so that at $\Pi^* = (\tilde{\Pi}^*, \pi^*)$, the directional derivative of $\sigma_1 - \sigma_2$ in the π-direction is nonzero. To simplify the notation, we fix all values of the system parameters except π, i.e., we fix $\tilde{\Pi} = \tilde{\Pi}^*$. We write (3.18)–(3.20) as

$$\dot{U} = G(U, w, \sigma, \pi), \tag{7.1}$$

$$\dot{V} = H(V, w, \sigma, \pi), \tag{7.2}$$

$$\dot{w} = q(v - u), \tag{7.3}$$

$$\dot{\sigma} = 0, \tag{7.4}$$

$$\dot{\pi} = 0. \tag{7.5}$$

In this formulation, $UVw\sigma\pi$-space is the state space, and q is a parameter. We now regard σ_1 and σ_2 as functions of π, so that $\sigma^* = \sigma_1(\pi^*) = \sigma_2(\pi^*)$. Our assumption that the directional derivative of $\sigma_1 - \sigma_2$ in the π-direction is nonzero becomes

$$(\sigma_1 - \sigma_2)'(\pi^*) \neq 0. \tag{7.6}$$

We shall also write the system (7.1)–(7.3) as

$$\dot{X} = F(X, \sigma, \pi, q) = \big(G(U, w, \sigma, \pi), H(V, w, \sigma, \pi), q(v - u) \big). \tag{7.7}$$

In this formulation, UVw-space is the state space, and σ, π, and q are parameters.

With q regarded as small, the system (7.1)–(7.5) is a singular perturbation problem in 7-dimensional $UVw\sigma\pi$-space, written in the fast time ξ. In the slow time $\tau = q\xi$, using prime to denote derivative with respect to τ, the system becomes

$$qU' = G(U, w, \sigma, \pi), \tag{7.8}$$

$$qV' = H(V, w, \sigma, \pi), \tag{7.9}$$

$$w' = v - u, \tag{7.10}$$

$$\sigma' = 0, \tag{7.11}$$

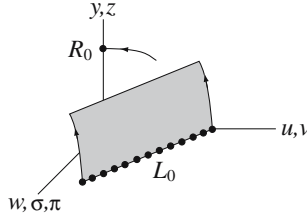$$\pi' = 0. \tag{7.12}$$

Figure 4. $W^u(L_0)$ and $W^s(R_0)$.

Let us consider the physically relevant region $0 \leqslant y \leqslant 1$, $0 \leqslant z \leqslant 1$. From Section 5, for $q = 0$ the equilibria of the fast systems (7.1)–(7.5) in this region include the following manifolds:

$$L_0 = \left\{ (u, y, v, z, w, \sigma, \pi) : u = u_L(w, \sigma, \pi) = \frac{\sigma d_1 - A_1 w}{A_1(\sigma a_1 - c_1)}, \right.$$
$$\left. v = v_L(w, \sigma, \pi) = \frac{\sigma d_2 + A_2 w}{A_2(\sigma a_2 - c_2)}, \ y = z = 0 \right\},$$
$$R_0 = \{ (u, y, v, z, w, \sigma, \pi) : u = v = w = 0 \text{ and } y = z = 1 \}$$

(see Figure 4). L_0 has dimension 3 and R_0 has dimension 2. From Section 5, equilibria in L_0 have four nonzero eigenvalues, two positive and two negative. Therefore, L_0 is a normally hyperbolic invariant manifold, and $W^u(L_0)$ has dimension 5. Equilibria in R_0 have two nonzero eigenvalues, both negative. Therefore, $W^s(R_0)$ has dimension 4.

The system $\dot{U} = G(U, 0, \sigma, \pi)$ has a strong connection from $(u_L(0, \sigma, \pi), 0)$ to $(0, 1)$ if and only if $\sigma = \sigma_1(\pi)$, and $\dot{V} = H(V, 0, \sigma, \pi)$ has a strong connection from $(v_L(0, \sigma, \pi), 0)$ to $(0, 1)$ if and only if $\sigma = \sigma_2(\pi)$.

Let $u_L^* = u_L(0, \sigma^*, \pi^*)$, $v_L^* = v_L(0, \sigma^*, \pi^*)$. Let $U^*(\xi) = (u^*(\xi), y^*(\xi))$ denote the connection of $\dot{U} = G(U, 0, \sigma^*, \pi^*)$ from $(u_L^*, 0)$ to $(0, 1)$, and let $V^*(\xi)) = (v^*(\xi), z^*(\xi))$ denote the connection of $\dot{V} = H(V, 0, \sigma^*, \pi^*)$ from $(v_L^*, 0)$ to $(0, 1)$ Then $\dot{X} = F(X, \sigma^*, \pi^*, 0)$ has a 2-dimensional sheet of traveling waves from $(u_L^*, 0, v_L^*, 0, 0)$ to $(0, 1, 0, 1, 0)$ given by

$$(U, V, w) = (U^*(\xi), V^*(\xi + \eta), 0). \tag{7.13}$$

$W^u(L_0)$ and $W^s(R_0)$ meet transversally along this 2-dimensional manifold; this is a consequence of (7.6) and will be shown in Section 8.

On L_0, the slow system (7.8)–(7.12) takes the form

$$w' = v_L(w, \sigma, \pi) - u_L(w, \sigma, \pi), \tag{7.14}$$
$$\sigma' = 0, \tag{7.15}$$
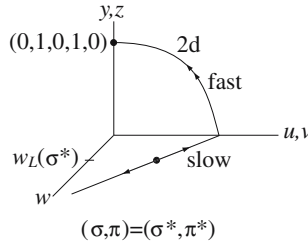$$\pi' = 0. \tag{7.16}$$

Figure 5. A singular solution.

From (5.3), the equation $w' = v_L(w, \sigma, \pi) - u_L(w, \sigma, \pi) = 0$ can be solved for w in terms of (σ, π): $w = w_L(\sigma, \pi)$. This equation defines a two-dimensional manifold of equilibria of (7.14)–(7.16) in $w\sigma\pi$-space. Since the coefficient of w in (5.3) is positive, the equilibria are normally repelling within $w\sigma\pi$-space. Let E_0 be the set of points in L_0 such that $w = w_L(\sigma, \pi)$, a two-dimensional manifold. More precisely, let $u_L(\sigma, \pi) = u_L(w_L(\sigma, \pi), \sigma, \pi)$; then

$$E_0 = \{(u, y, v, z, w, \sigma, \pi) : u = v = u_L(\sigma, \pi), \, y = z = 0, \, w = w_L(\sigma, \pi)\}.$$

All points in E_0 have $u = v > 0$. We saw in Section 5 that points of E_0 remain equilibria for $q > 0$.

Let $w^* = w_L(\sigma^*, \pi^*)$. For $q = 0$ we have the following singular solutions of the singular perturbation problem (7.1)–(7.5):

(1) Slow part: the solution of (7.14)–(7.16) from (w^*, σ^*, π^*) to $(0, \sigma^*, \pi^*)$. In $uyvzw\sigma\pi$-space, this solution goes from $\big(u_L(w^*, \sigma^*, \pi^*), 0, u_L(w^*, \sigma^*, \pi^*), 0, w^*, \sigma^*, \pi^*\big)$ to $(u_L^*, 0, v_L^*, 0, 0, \sigma^*, \pi^*)$.
(2) Fast part: one of the connecting orbits (7.13) from $(u_L^*, 0, v_L^*, 0, 0, \sigma^*, \pi^*)$ to $(0, 1, 0, 1, 0, \sigma^*, \pi^*)$

(see Figure 5). We are interested in solutions for small $q > 0$ near these singular solutions.

The fast part of the singular solution represents combustion. Along the slow part of the singular solution, y and z are 0, i.e., there is no reactant left; the temperatures u and v slowly change.

For fixed small $q > 0$, R_0 persists as a 2-dimensional set of equilibria R_q of the fast system (7.1)–(7.5), given by the same equations. For small $q > 0$, we saw in Section 4 that equilibria in R_q have three nonzero eigenvalues, one small positive and two negative. Therefore, $W^s(R_q)$ has dimension 4 and is close to $W^s(R_0)$.

For fixed small $q > 0$, there is a normally hyperbolic invariant manifold L_q near L_0, given by equations of the form

$$u = \tilde{u}_L(w, p) = u_L(w, \sigma, \pi) + O(q),$$
$$y = 0,$$
$$v = \tilde{v}_L(w, p) = v_L(w, \sigma, \pi) + O(q),$$
$$z = 0.$$

$W^u(L_q)$ of course still has dimension 5. L_q contains the 2-dimensional sheet of equilibria E_0, so

$$\tilde{u}_L\big(w_L(\sigma, \pi), \sigma, \pi, q\big) = u_L\big(w_L(\sigma, \pi), \sigma, \pi\big) = u_L(\sigma, \pi).$$

To lowest order in q, the flow on L_q in the slow time is given by (7.14)–(7.16). For the fast system (7.1)–(7.5) with $q > 0$, equilibria in E_q are weakly repelling within L_q.

$W^u(L_0)$ and $W^s(R_0)$ meet transversally in the two-dimensional manifold (7.13). Therefore, for small $q > 0$, $W^u(L_q)$ and $W^s(R_q)$ meet transversally in a 2-dimensional sheet of orbits that connect L_q to R_q. Upon arrival near L_q in backwards time, each of these orbits shadows a solution in L_q, which in backwards time approaches an equilibrium in E_0. Thus each solution in $W^u(L_q) \cap W^s(R_q)$ connects a left state $(u_L, 0, u_L, 0, w_L, \sigma, \pi)$ to the right state $(0, 1, 0, 1, 0, \sigma, \pi)$. Such a connection moves slowly from $(u_L, 0, u_L, 0, w_L, \sigma, \pi)$ to approximately $(u_L^*, 0, v_L^*, 0, 0, \sigma, \pi)$, then jumps quickly to $(0, 1, 0, 1, 0, \sigma, \pi)$.

For $q = 0$, the connecting orbits all occur for one value of π. For $q > 0$, this is not the case. We shall show in Section 8 that for small $q > 0$, traveling waves occur for an interval of values of π near π^*.

Our argument relies on the following observation. One can define a function that measures the separation between $W^u(L_q)$ and $W^s(R_q)$ near a point on one of the connecting orbits (7.13). Its derivative with respect to q at $q = 0$ is a Melnikov integral, which is the integral along the connecting orbit of the product of a solution of a certain adjoint linear differential equation with $\frac{\partial F}{\partial q}$. The w-component of $\frac{\partial F}{\partial q}$ is $v - u$. If the connecting orbit has η large positive, then the vz-component of the orbit arrives near $(0, 1)$ while the uy-component is still near $(u_L, 0)$. The orbit then spends a long time with (u, y, v, z) near $(u_L, 0, 0, 1)$, where $v - u$ is large negative. Thus the Melnikov integral becomes large as $\eta \to \infty$. A similar phenomenon occurs as $\eta \to -\infty$.

We note that for $q = 0$, a connecting orbit with η large positive looks like a connection from $(v_L, 0)$ to $(0, 1)$ in vz-space, followed by a connection from $(u_L, 0)$ to $(0, 1)$ in uy-space. For small $q > 0$, nearby connecting
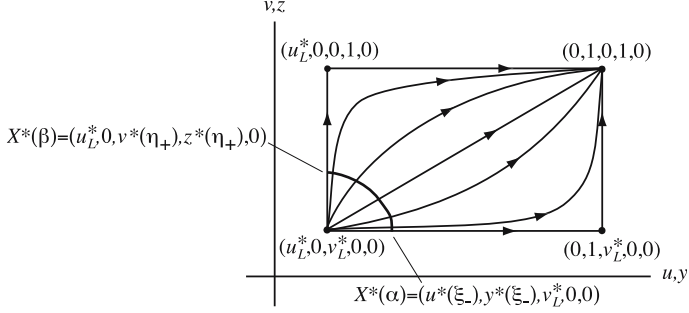
Figure 6. The two-dimensional manifold of connecting orbits from $(u_L^*, 0, v_L^*, 0, 0)$ to $(0, 1, 0, 1, 0)$ for $(\sigma, \pi, q) = (\sigma^*, \pi^*, 0)$. The curve $X^*(\zeta)$, $\alpha \leqslant \zeta \leqslant \beta$, is in the lower left. The picture shows the plane $w = 0$, which contains all the connecting orbits.

orbits retain this form. Thus the combustion front in uy-space occurs to the left of the combustion front in vz-space.

8. SEPARATION FUNCTION AND MELNIKOV INTEGRALS

In this section, we construct the separation function between $W^u(L_q)$ and $W^s(R_q)$, derive formulas for its derivatives as Melnikov integrals, estimate the integrals, and show how the result implies Theorem 7.1. We give full details since our situation has two nonstandard aspects occurring simultaneously: (1) nonhyperbolic equilibria; and (2) a two-dimensional sheet of connecting orbits when $q = 0$, made up of two basic solutions with arbitrary phase shift between them. The first degeneracy is treated in [4, 16]. The latter situation occurs in [2]; in fact, Figure 6 below also appears in [2]. (This paper was discussed in Section 1.)

This section is organized as follows. In Section 8.1, we construct the separation function. The results to be proved are stated in Section 8.2. They are proved in the remaining Sections.

In this section, we treat q as a state variable. Thus we consider the extended system

$$\dot{X} = F(X, \sigma, \pi, q), \quad \dot{\sigma} = \dot{\pi} = \dot{q} = 0 \tag{8.1}$$

on 8-dimensional $X\sigma\pi q$-space. Let L (respectively, R) denote the set of (X, σ, π, q) such that (X, σ, π) is in L_q (respectively, R_q). Where convenient, we shall simplify the notation by writing $p = (\sigma, \pi, q)$ and $p^* = (\sigma^*, \pi^*, 0)$; σ^* and π^* were defined in the previous section.

8.1. Construction of the Separation Function Between $W^u(L_q)$ and $W^s(R_q)$

We first define $\big(\xi^*(\zeta), \eta^*(\zeta)\big)$, $\alpha < \zeta < \beta$, so that the curve

$$X^*(\zeta) = \Big(U^*\big(\xi^*(\zeta)\big), V^*\big(\xi^*(\zeta) + \eta^*(\zeta)\big), 0\Big)$$

satisfies

(X1) $\|X^{*\prime}(\zeta)\| = 1$,
(X2) $X^{*\prime}(\zeta) \cdot F\big(X^*(\zeta), \sigma^*, \pi^*, 0\big) = 0$,
(X3) $\lim_{\zeta \to \alpha} \xi^*(\zeta) = \xi_-$,
(X4) $\lim_{\zeta \to \alpha} \eta^*(\zeta) = -\infty$,
(X5) $\lim_{\zeta \to \beta} \xi^*(\zeta) = -\infty$,
(X6) $\lim_{\zeta \to \beta} \xi^*(\zeta) + \eta^*(\zeta) = \eta_+$

with ξ_- and η_+ finite (see Figure 6). From (X5) and (X6),

(X7) $\lim_{\zeta \to \beta} \eta^*(\zeta) = \infty$.

We extend $X^*(\zeta)$ to $\alpha \leqslant \zeta \leqslant \beta$ by setting $X^*(\alpha) = \big(U^*(\xi_-), 0, 0\big)$ and $X^*(\beta) = \big(0, V^*(\eta_+), 0\big)$.
Let

$$a(\zeta) = \big\|\dot{U}^*\big(\xi^*(\zeta)\big)\big\|^{-1}, \quad U_3(\zeta) = a(\zeta)\Big(-\dot{y}^*\big(\xi^*(\zeta)\big), \dot{u}^*\big(\xi^*(\zeta)\big)\Big),$$

$$b(\zeta) = \big\|\dot{V}^*\big(\xi^*(\zeta) + \eta^*(\zeta)\big)\big\|^{-1},$$

$$V_4(\zeta) = b(\zeta)\Big(-\dot{z}^*\big(\xi^*(\zeta) + \eta^*(\zeta)\big), \dot{v}^*\big(\xi^*(\zeta) + \eta^*(\zeta)\big)\Big),$$

$$X_3(\zeta) = \big(U_3(\zeta), 0, 0\big), \quad X_4(\zeta) = \big(0, V_4(\zeta), 0\big), \quad X_5 = (0, 0, 1).$$

We have $\lim_{\zeta \to \beta} a(\zeta) = \infty$ and $\lim_{\zeta \to \alpha} b(\zeta) = \infty$. The vectors $U_3(\zeta)$ and $V_4(\zeta)$ have norm 1. The definitions of U_3 and V_4 extend to to $\zeta = \alpha$ and $\zeta = \beta$ by continuity. The vector $U_3(\beta)$ (respectively, $U_4(\alpha)$) is orthogonal to the unstable eigenvector of $DG(u_L^*, 0, 0, \sigma^*, \pi^*)$ (respectively, the unstable eigenvector of $DH(v_L^*, 0, 0, \sigma^*, \pi^*)$).
We define a 4-dimensional cross-section Σ to the flow in X-space to be the image of the the map

$$\Phi(\zeta, \gamma, \delta, \omega) = X^*(\zeta) + \gamma X_3(\zeta) + \delta X_4(\zeta) + \omega X_5.$$

A portion of the 5-dimensional manifold $W^s(R)$ can be parameterized as $(X^s(\xi; \zeta, p), p)$, with each curve $X = X^s(\cdot; \zeta, p)$ a solution of (7.7), and

$$X^s\big(\xi^*(\zeta); \zeta, p\big) = X^*(\zeta) + \gamma^s(\zeta, p)X_3(\zeta) + \delta^s(\zeta, p)X_4(\zeta) + w^s(\zeta, p)X_5.$$

Then $\gamma^s(\zeta, p^*) = \delta^s(\zeta, p^*) = 0$ and $w^s(\zeta, \sigma, \pi, 0) = 0$.

A portion of the 6-dimensional manifold $W^u(L)$ can be parameterized as $(X^u(\xi; \zeta, \omega, p), p)$, with each curve $X = X^u(\cdot; \zeta, \omega, p)$ a solution of (7.7) and

$$X^u\big(\xi^*(\zeta); \zeta, \omega, p\big) = X^*(\zeta) + \gamma^u(\zeta, \omega, p)X_3(\zeta) + \delta^u(\zeta, \omega, p)X_4(\zeta)$$
$$+ w^u(\zeta, \omega, p)X_5.$$

Then $\gamma^u(\zeta, 0, p^*) = \delta^u(\zeta, 0, p^*) = 0$, and we may assume that $w^u(\zeta, \omega, \sigma, \pi, 0) = \omega$. We may assume:

(X8) For each (ω, p), the curve $X^u\big(\xi^*(\zeta); \zeta, \omega, p\big)$ lies in the unstable fiber of the point $\big(\tilde{u}_L(\omega, p), 0, \tilde{v}_L(\omega, p), 0, \omega, p\big)$ in L.

The functions $\tilde{u}$ and $\tilde{v}$ were defined in the previous section. Note that (X8) holds automatically for $q = 0$.

Let

$$\tilde{X}^u(\zeta_L, \omega, p) = \Phi^{-1} \circ X^u\big(\xi^*(\zeta_L); \zeta_L, \omega, p\big), \tag{8.2}$$
$$\tilde{X}^s(\zeta_R, p) = \Phi^{-1} \circ X^s\big(\xi^*(\zeta_R); \zeta_R, p\big), \tag{8.3}$$
$$\tilde{S}(\zeta_L, \omega, \zeta_R, p) = \tilde{X}^u(\zeta_L, \omega, p) - \tilde{X}^s(\zeta_R, p). \tag{8.4}$$

Φ^{-1} is of course a mapping from Σ to $\zeta\gamma\delta\omega$-space. The function $\tilde{S}$, from $\zeta_L\omega\zeta_R\sigma\pi q$-space to $\zeta\gamma\delta\omega$-space, measures the separation between points of $W^u(L)$ and $W^s(R)$ in the the cross-section Σ.

Connecting orbits from from L to R are in one-to-one correspondence with solutions of the equation $\tilde{S} = 0$. We will first solve the system $\tilde{S}_1 = \tilde{S}_4 = 0$ for (ζ_L, ω) in terms of (ζ_R, p). We have

$$\tilde{S}_1(\zeta_L, \omega, \zeta_R, p) = \zeta_L - \zeta_R \quad \text{and} \quad \tilde{S}_4(\zeta_L, \omega, \zeta_R, \sigma, \pi, 0) = \omega - 0 = \omega.$$

Therefore, $\zeta_L = \zeta_R$, and, by the implicit function theorem, $\omega = \omega(\zeta_R, p)$, with $\omega(\zeta_R, \sigma, \pi, 0) = 0$.

Let

$$S_i(\zeta_R, p) = \tilde{S}_{i+1}\big(\zeta_R, \omega(\zeta_R, p), \zeta_R, p\big), \quad i = 1, 2$$

and let $S = (S_1, S_2)$. S is the *separation function* between $W^u(L)$ and $W^s(R)$. Solutions of $\tilde{S} = 0$ are in one-to-one correspondence with solutions of $S = 0$.
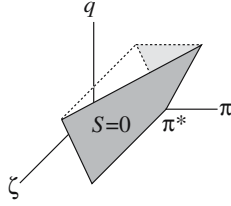
Figure 7. A portion of the surface $S = 0$ and its projection to πq-space. In the picture, $\frac{\partial \pi}{\partial q}(\zeta, 0)$ is negative for large ζ and positive for small ζ. The variable σ has been suppressed.

8.2. Statement of Results

We have $S(\zeta, \sigma^*, \pi^*, 0) = 0$. We wish to find $\big(\sigma(\zeta, q), \pi(\zeta, q)\big)$ such that $\big(\sigma(\zeta, 0), \pi(\zeta, 0)\big) = (\sigma^*, \pi^*)$ and

$$S\big(\zeta, \sigma(\zeta, q), \pi(\zeta, q), q\big) = 0. \tag{8.5}$$

According to the implicit function theorem, this can be done provided

$$D(\zeta) = \frac{\partial S_1}{\partial \sigma}(\zeta, p^*) \frac{\partial S_2}{\partial \pi}(\zeta, p^*) - \frac{\partial S_1}{\partial \pi}(\zeta, p^*) \frac{\partial S_2}{\partial \sigma}(\zeta, p^*) \tag{8.6}$$

is not zero.

> **Proposition 8.1.** $D(\zeta) \neq 0$.

In the course of the proof we will derive a useful formula for $D(\zeta)$. This proposition implies the following result, which was stated in the previous section.

> **Corollary 8.2.** $W^u(L_0)$ and $W^s(R_0)$ meet transversally along the 2-dimensional manifold given by (7.13).

For fixed q, a traveling wave exists for a value of π provided π is in the range of the function $\pi(\zeta, q)$ (see Figure 7).

> **Theorem 8.3.** As $\zeta \to \alpha$, $\frac{\partial \pi}{\partial q}(\zeta, 0) \to \infty$, and as $\zeta \to \beta$, $\frac{\partial \pi}{\partial q}(\zeta, 0) \to -\infty$; or the reverse. In particular, for small $q > 0$, the range of $\pi(\zeta, q)$ includes an open interval.

This result implies Theorem 7.1.

The remainder of this section is devoted to the proofs of these results. Formulas for partial derivatives of the separation function are needed in the proofs; we begin their derivation in Section 8.3 and complete it in Section 8.4. In Section 8.5, these formulas are used to prove Proposition 8.1

and Corollary 8.2. In Section 8.6, we prove Theorem 8.3 by deriving and estimating an integral formula for $\frac{\partial \pi}{\partial q}(\zeta, 0)$.

8.3. Partial Derivatives of the Separation Function: Introduction

For $r = \sigma$, π or q, and $i = 1, 2$, we have

$$
\begin{aligned}
\frac{\partial S_i}{\partial r}(\zeta, p^*) &= \frac{\partial \tilde{S}_{i+1}}{\partial \omega}(\zeta, 0, \zeta, p^*)\frac{\partial \omega}{\partial r}(\zeta, p^*) + \frac{\partial \tilde{S}_{i+1}}{\partial r}(\zeta, 0, \zeta, p^*) \\
&= \frac{\partial \tilde{S}_{i+1}}{\partial r}(\zeta, 0, \zeta, p^*).
\end{aligned}
\tag{8.7}
$$

Therefore, we study $D\tilde{S}(\zeta, 0, \zeta, p^*)$.

We have

$$
D\tilde{S}(\zeta, 0, \zeta, p^*) = D\Phi^{-1}\big(X^*(\zeta)\big)\{DX^u\big(\xi^*(\zeta); \zeta, 0, p^*\big) - DX^s\big(\xi^*(\zeta); \zeta, p^*\big)\}.
\tag{8.8}
$$

Let

$$
k(\zeta) = \xi^{*\prime}(\zeta), \quad \ell(\zeta) = \xi^{*\prime}(\zeta) + \eta^{*\prime}(\zeta), \quad c(\zeta) = \frac{\partial \gamma^u}{\partial \omega}(\zeta, 0, p^*),
$$

$$
d(\zeta) = \frac{\partial \gamma^s}{\partial \omega}(\zeta, 0, p^*).
$$

Then

$$
D\Phi(\zeta, 0, 0, 0) = \Big(X^{*\prime}(\zeta) \ \ \frac{\partial X^u}{\partial \omega}\big(\xi^*(\zeta); \zeta, 0, p^*\big) \ \ X_3(\zeta) \ \ X_4(\zeta)\Big)
$$

$$
= \begin{pmatrix}
k(\zeta)\dot{u}^*\big(\xi^*(\zeta)\big) & -a(\zeta)\dot{y}^*\big(\xi^*(\zeta)\big) & 0 & -c(\zeta)a(\zeta)\dot{y}^*\big(\xi^*(\zeta)\big) \\
k(\zeta)\dot{y}^*\big(\xi^*(\zeta)\big) & a(\zeta)\dot{u}^*\big(\xi^*(\zeta)\big) & 0 & c(\zeta)a(\zeta)\dot{u}^*\big(\xi^*(\zeta)\big) \\
\ell(\zeta)\dot{v}^*\big(\xi^*(\zeta)+\eta^*(\zeta)\big) & 0 & -b(\zeta)\dot{z}^*\big(\xi^*(\zeta)+\eta^*(\zeta)\big) & -d(\zeta)b(\zeta)\dot{z}^*\big(\xi^*(\zeta)+\eta^*(\zeta)\big) \\
\ell(\zeta)\dot{z}^*\big(\xi^*(\zeta)+\eta^*(\zeta)\big) & 0 & b(\zeta)\dot{v}^*\big(\xi^*(\zeta)+\eta^*(\zeta)\big) & d(\zeta)b(\zeta)\dot{v}^*\big(\xi^*(\zeta)+\eta^*(\zeta)\big) \\
0 & 0 & 0 & 1
\end{pmatrix}.
\tag{8.9}
$$

The first three columns of (8.9) have norm 1. Therefore,

$$
D\Phi^{-1}(X^*(\zeta))
$$

$$
= \begin{pmatrix}
k(\zeta)\dot{u}^*\big(\xi^*(\zeta)\big) & k(\zeta)\dot{y}^*\big(\xi^*(\zeta)\big) & \ell(\zeta)\dot{v}^*\big(\xi^*(\zeta)+\eta^*(\zeta)\big) & \ell(\zeta)\dot{z}^*\big(\xi^*(\zeta)+\eta^*(\zeta)\big) & 0 \\
-a(\zeta)\dot{y}^*\big(\xi^*(\zeta)\big) & a(\zeta)\dot{u}^*\big(\xi^*(\zeta)\big) & 0 & 0 & -c(\zeta) \\
0 & 0 & -b(\zeta)\dot{z}^*\big(\xi^*(\zeta)+\eta^*(\zeta)\big) & b(\zeta)\dot{v}^*\big(\xi^*(\zeta)+\eta^*(\zeta)\big) & -d(\zeta) \\
0 & 0 & 0 & 0 & 1
\end{pmatrix}.
\tag{8.10}
$$

Consider the linear differential equation with parameter ζ

$$\dot{Y}(\xi) = D_X F\left(U^*(\xi), V^*\big(\xi + \eta^*(\zeta)\big), 0, p^*\right) Y(\xi)$$

with $D_X F$ given by (5.5). Denote the solution by $Y(\xi) = \Psi(\xi, \xi_0; \zeta) Y(\xi_0)$. Now consider the adjoint differential equation with parameter ζ:

$$\dot{\psi}(\xi) = -\psi(\xi) D_X F\left(U^*(\xi), V^*\big(\xi + \eta^*(\zeta)\big), 0, p^*\right).$$

We denote the solution whose value at $\xi = \xi^*(\zeta)$ is the third (respectively, fourth) row of $D\Phi^{-1}(X^*(\zeta))$ by $\psi_1(\xi; \zeta)$ (respectively, $\psi_2(\xi; \zeta)$).

The following proposition collects useful facts.

Proposition 8.4. (1) $\psi_1(\xi; \zeta) = \big(\psi_{11}(\xi; \zeta)\ \psi_{12}(\xi; \zeta)\ 0\ 0\ \psi_{15}(\xi; \zeta)\big)$ with

$$\big(\psi_{11}(\xi; \zeta)\ \psi_{12}(\xi; \zeta)\big) = a(\zeta) \exp\left(-\int_{\xi^*(\zeta)}^{\xi} div\ G\big(U^*(\tau), 0, \sigma^*, \pi^*\big)\, d\tau\right)$$
$$\times \big(-\dot{y}^*(\xi)\ \dot{u}^*(\xi)\big).$$

(2) $c(\zeta) = \int_{-\infty}^{\xi^*(\zeta)} \big(\psi_{11}(\xi; \zeta)\ \psi_{12}(\xi; \zeta)\big) \frac{\partial G}{\partial w}\big(U^*(\xi), 0, \sigma^*, \pi^*\big)\, d\xi$
$= -\int_{-\infty}^{\xi^*(\zeta)} \psi_{11}(\xi; \zeta) \cdot \frac{1}{\lambda_1}\, d\xi.$

(3) $\psi_{15}(\xi; \zeta) = -c(\zeta) + \int_{\xi^*(\zeta)}^{\xi} \psi_{11}(\tau; \zeta) \cdot \frac{1}{\lambda_1}\, d\tau = \int_{-\infty}^{\xi} \psi_{11}(\tau; \zeta) \cdot \frac{1}{\lambda_1}\, d\tau.$

(4) $\psi_2(\xi; \zeta) = \big(0\ 0\ \psi_{23}(\xi; \zeta)\ \psi_{24}(\xi; \zeta)\ \psi_{25}(\xi; \zeta)\big)$ with $\big(\psi_{23}(\xi; \zeta)\ \psi_{24}(\xi; \zeta)\big) =$

$$b(\zeta) \exp\left(-\int_{\xi^*(\zeta)}^{\xi} div\ H\big(V^*(\tau + \eta^*(\zeta)), 0, \sigma^*, \pi^*\big)\, d\tau\right)$$
$$\big(-\dot{z}^*(\xi + \eta^*(\zeta))\ \dot{v}^*(\xi + \eta^*(\zeta))\big).$$

(5) $d(\zeta) = \int_{-\infty}^{\xi^*(\zeta)} \big(\psi_{23}(\xi; \zeta)\ \psi_{24}(\xi; \zeta)\big) \frac{\partial H}{\partial w}\big(V^*(\xi + \eta^*(\zeta)), 0, \sigma^*, \pi^*\big)\, d\xi$
$= \int_{-\infty}^{\xi^*(\zeta)} \psi_{23}(\xi; \zeta) \cdot \frac{1}{\lambda_2}\, d\xi.$

(6) $\psi_{25}(\xi; \zeta) = -d(\zeta) - \int_{\xi^*(\zeta)}^{\xi} \psi_{23}(\tau; \zeta) \cdot \frac{1}{\lambda_2}\, d\tau = -\int_{-\infty}^{\xi} \psi_{23}(\tau; \zeta) \cdot \frac{1}{\lambda_2}\, d\tau.$

(7) As $\xi \to -\infty$, all $\psi_{ij}(\xi; \zeta)$ go to 0 exponentially. As $\xi \to \infty$, $\psi_{11}(\xi; \zeta)$ and $\psi_{23}(\xi; \zeta)$ go to 0; $\psi_{12}(\xi; \zeta)$, $\psi_{15}(\xi; \zeta)$, $\psi_{24}(\xi; \zeta)$, and $\psi_{25}(\xi; \zeta)$ approach constants.

Proof. (1) and (4) follow from the formula (5.5). (Compare (4.14).) (2) and (5) follow from standard Melnikov integral calculations. Then (3) and (6) follow from the formula (5.5).

To prove (7), let $-\nu_{u_L}$ denote the negative eigenvalue of $DG(0, 1, 0, \sigma^*, \pi^*)$. Since the corresponding eigenvector is horizontal, we have

$$\lim_{\xi \to \infty} e^{\nu_{u_L}\xi} \big(\dot{u}(\xi), \dot{y}(\xi)\big) = (-K, 0)$$

for some $K > 0$. Also, as $\xi \to \infty$, div $G\big(U^*(\xi), 0, \sigma^*, \pi^*\big) = -\nu_{u_L} + O(e^{-\nu_{u_L}\xi})$. It follows that as $\xi \to \infty$, $\psi_{11}(\xi; \zeta) \to 0$, and $\psi_{12}(\xi; \zeta)$ and $\psi_{25}(\xi; \zeta)$ approach constants. The other parts of (7) rely on similar arguments. $\qquad\square$

8.4. Partial Derivatives of the Separation Function: Formulas

Proposition 8.5. For $r = \sigma$, π, or q, $\frac{\partial S_i}{\partial r}(\zeta, p^*) = \int_{-\infty}^{\infty} \psi_i(\xi; \zeta) \frac{\partial F}{\partial r}\big(U^*(\xi), V^*(\xi + \eta^*(\zeta)), 0, p^*\big) d\xi$.

Proof. From (8.7), (8.8), and (8.10), we have

$$DS(\zeta, p^*) = \begin{pmatrix} \psi_1\big(\xi^*(\zeta); \zeta\big) \\ \psi_2\big(\xi^*(\zeta); \zeta\big) \end{pmatrix} \{DX^u\big(\xi^*(\zeta); \zeta, 0, p^*\big) - DX^s\big(\xi^*(\zeta); \zeta, p^*\big)\}.$$

$$(8.11)$$

For $r = \sigma$, π, or q,

$$\frac{\partial}{\partial \xi} \frac{\partial X^u}{\partial r} = \frac{\partial}{\partial r} \frac{\partial X^u}{\partial \xi} = \frac{\partial}{\partial r} F(X^u, p).$$

Therefore, $\frac{\partial X^u}{\partial r}(\xi; \zeta, 0, p^*)$ satisfies

$$\dot{Y} = D_X F\big(U^*(\xi), V^*(\xi + \eta^*(\zeta)), 0, p^*\big)Y + \frac{\partial F}{\partial r}\big(U^*(\xi), V^*(\xi+\eta^*(\zeta)), 0, p^*\big).$$

Then for any ξ_0 we have

$$\frac{\partial X^u}{\partial r}\big(\xi^*(\zeta); \zeta, 0, p^*\big)$$
$$= \Psi\big(\xi^*(\zeta), \xi_0; \zeta\big)\frac{\partial X^u}{\partial r}(\xi_0; \zeta, 0, p^*)$$
$$+ \int_{\xi_0}^{\xi^*(\zeta)} \Psi\big(\xi^*(\zeta), \xi; \zeta\big)\frac{\partial F}{\partial r}\big(U^*(\xi), V^*(\xi + \eta^*(\zeta)), 0, p^*\big) d\xi.$$

$$(8.12)$$

Multiplying (8.12) by $\psi_i\big(\xi^*(\zeta); \zeta\big)$, we obtain

$$\psi_i\big(\xi^*(\zeta); \zeta\big)\frac{\partial X^u}{\partial r}\big(\xi^*(\zeta); \zeta, 0, p^*\big)$$
$$= \psi_i(\xi_0; \zeta)\frac{\partial X^u}{\partial r}(\xi_0; \zeta, 0, p^*)$$
$$+ \int_{\xi_0}^{\xi^*(\zeta)} \psi_i(\xi; \zeta)\frac{\partial F}{\partial r}\big(U^*(\xi), V^*(\xi + \eta^*(\zeta)), 0, p^*\big) d\xi. \quad (8.13)$$

Similarly,

$$\psi_i\big(\xi^*(\zeta);\zeta\big)\frac{\partial X^s}{\partial r}\big(\xi^*(\zeta);\zeta,p^*\big)$$

$$=\psi_i(\xi_1;\zeta)\frac{\partial X^s}{\partial r}(\xi_1;\zeta,p^*)$$

$$+\int_{\xi_1}^{\xi^*(\zeta)}\psi_i(\xi;\zeta)\frac{\partial F}{\partial r}\Big(U^*(\xi),V^*\big(\xi+\eta^*(\zeta)\big),0,p^*\Big)d\xi. \quad (8.14)$$

From (8.11), (8.13), and (8.14),

$$\frac{\partial S_i}{\partial r}(\zeta,p^*)=\lim_{(\xi_0,\xi_1)\to(-\infty,\infty)}\Big(\psi_i(\xi_0;\zeta)\frac{\partial X^u}{\partial r}(\xi_0;\zeta,0,p^*)-\psi_i(\xi_1;\zeta)\frac{\partial X^s}{\partial r}(\xi;\zeta,p^*)$$

$$+\int_{\xi_0}^{\xi_1}\psi_i(\xi;\zeta)\frac{\partial F}{\partial r}\Big(U^*(\xi),V^*\big(\xi+\eta^*(\zeta)\big),0,p^*\Big)d\xi\Big). \quad (8.15)$$

For $r=\sigma$, π, or q, as $\xi\to\infty$, $\frac{\partial X^s}{\partial r}(\xi;\zeta,p^*)$ approaches 0 exponentially, since the equilibrium is always $(0,1,0,1,0)$. Then from Proposition 8.4 (7) the limit of the second term in (8.15) is 0.

For $r=\sigma$ or π, as $\xi\to-\infty$, $\frac{\partial X^u}{\partial r}(\xi;\zeta,0,p^*)$ approaches exponentially the vector $\big(\frac{\partial u_L}{\partial r}(0,\sigma^*,\pi^*),0,\frac{\partial v_L}{\partial r}(0,\sigma^*,\pi^*),0,0\big)$. Then from Proposition 8.4 (7) the limit of the first term in (8.15) is 0.

For $r=q$, this term requires a more detailed treatment. From (X8), as $\xi\to-\infty$, the solutions $X^u(\xi;\zeta,\omega,p)$ approach exponentially solutions $X_L(\xi-\xi^*(\zeta);\omega,p)$ in L. We have

$$X_L(\xi;\omega,\sigma,\pi,q)=X_L(\xi;\omega,\sigma,\pi,0)+O(q)$$

$$=\big(u_L(\omega,\sigma,\pi),0,v_L(\omega,\sigma,\pi),0,\omega\big)$$

$$+q\big(\hat{u}_L(\xi;\omega,\sigma,\pi),0,\hat{v}_L(\xi;\omega,\sigma,\pi),0,\hat{w}_L(\xi;\omega,\sigma,\pi)\big)$$

$$+O(q^2).$$

We find that

$$\frac{\partial}{\partial\xi}\begin{pmatrix}\hat{u}_L(\xi;\omega,\sigma,\pi)\\ \hat{v}_L(\xi;\omega,\sigma,\pi)\\ \hat{w}_L(\xi;\omega,\sigma,\pi)\end{pmatrix}$$

$$=\begin{pmatrix}\frac{\partial G_1}{\partial u}\big(u_L(\omega,\sigma,\pi),0,\omega,\sigma,\pi\big) & 0 & \frac{\partial G_1}{\partial w}\big(u_L(\omega,\sigma,\pi),0,\omega,\sigma,\pi\big)\\ 0 & \frac{\partial H_1}{\partial v}\big(v_L(\omega,\sigma,\pi),0,\omega,\sigma,\pi\big) & \frac{\partial H_1}{\partial w}\big(v_L(\omega,\sigma,\pi),0,\omega,\sigma,\pi\big)\\ 0 & 0 & 0\end{pmatrix}$$

$$\cdot\begin{pmatrix}\hat{u}_L(\xi;\omega,\sigma,\pi)\\ \hat{v}_L(\xi;\omega,\sigma,\pi)\\ \hat{w}_L(\xi;\omega,\sigma,\pi)\end{pmatrix}+\begin{pmatrix}0\\ 0\\ v_L(\omega,\sigma,\pi)-u_L(\omega,\sigma,\pi)\end{pmatrix}.$$

From (X8), $\hat{w}_L(0; \omega, \sigma, \pi) = 0$. Therefore

$$\hat{w}_L(\xi - \xi^*(\zeta); \omega, \sigma, \pi) = (v_L(\omega, \sigma, \pi) - u_L(\omega, \sigma, \pi))(\xi - \xi^*(\zeta))$$

and there are constants a_L, b_L, c_L, d_L such that, for $\xi < 0$,

$$\hat{u}_L(\xi; \omega, \sigma, \pi) = a_L + b_L \xi + \text{exponentially small terms,}$$
$$\hat{v}_L(\xi; \omega, \sigma, \pi) = c_L + d_L \xi + \text{exponentially small terms.}$$

Also, as $\xi \to -\infty$, $\frac{\partial X^u}{\partial q}(\xi; \zeta, \omega, p)$ approaches exponentially $\frac{\partial X_L}{\partial q}(\xi - \xi^*(\zeta); \omega, p)$. Therefore, in (8.15) with $r = q$, for $\xi - \xi^*(\zeta) < 0$,

$$\frac{\partial X^u}{\partial q}(\xi_0; \zeta, 0, p^*) = \left(\hat{u}_L(\xi_0 - \xi^*(\zeta); 0, \sigma^*, \pi^*), 0, \hat{v}_L(\xi_0 - \xi^*(\zeta); 0, \sigma^*, \pi^*), \right.$$
$$\left. 0, (v_L^* - u_L^*)(\xi_0 - \xi^*(\zeta)) \right)$$

plus exponentially small terms.

Then from Proposition 8.4 (7) the limit of the second term in (8.15) is 0. $\qquad \square$

We now introduce notation to show the dependence of various quantities on ζ more explicitly. Define $\psi_1^*(\xi) = (\psi_{11}^*(\xi) \; \psi_{12}^*(\xi) \; 0 \; 0 \; \psi_{15}^*(\xi))$ with

$$(\psi_{11}^*(\xi) \; \psi_{12}(\xi)) = \exp\left(-\int_0^\xi \text{div } G(U^*(\tau), 0, \sigma^*, \pi^*) \, d\tau\right)(-\dot{y}^*(\xi) \; \dot{u}^*(\xi)),$$
$$\psi_{15}^*(\xi) = \frac{1}{\lambda_1} \int_{-\infty}^\xi \psi_{11}^*(\tau) \, d\tau.$$

Let

$$A(\zeta) = \exp \int_0^{\xi^*(\zeta)} \text{div } G(U^*(\tau), 0, \sigma^*, \pi^*) \, d\tau \quad \text{and}$$
$$M_r(\zeta) = \int_{-\infty}^\infty \psi_1^*(\xi) \frac{\partial G}{\partial r}(U^*(\xi), 0, p^*) \, d\xi.$$

$M_r(\zeta)$ is independent of ζ for $r = \sigma, \pi$. We have

$$\psi_1(\xi; \zeta) = a(\zeta) A(\zeta) \psi_1^*(\xi),$$

and, for $r = \sigma, \pi,$ or q,

$$\frac{\partial S_1}{\partial r}(\zeta, p^*) = \int_{-\infty}^\infty \psi_1(\xi; \zeta) \frac{\partial G}{\partial r}(U^*(\xi), 0, p^*) \, d\xi = a(\zeta) A(\zeta) M_r(\zeta).$$
$$(8.16)$$

Also, let $\eta = \xi + \eta^*(\xi)$, and define $\phi_2(\eta; \zeta) = \psi_2(\xi; \zeta)$. Define

$$\phi_2^*(\eta) = \begin{pmatrix} 0 & 0 & \phi_{23}^*(\eta) & \phi_{24}^*(\eta) & \phi_{25}^*(\eta) \end{pmatrix}$$

with

$$\left(\phi_{23}^*(\eta) \ \phi_{24}^*(\eta)\right) = \exp\left(-\int_0^\eta \operatorname{div} \ H\big(V^*(\theta), 0, \sigma^*, \pi^*\big) d\theta\right)\left(-\dot{z}^*(\eta) \ \dot{v}^*(\eta)\right),$$

$$\phi_{25}^*(\eta) = -\frac{1}{\lambda_2}\int_{-\infty}^\eta \phi_{23}^*(\theta) \, d\theta. \tag{8.17}$$

Let

$$B(\zeta) = \exp\int_0^{\xi^*(\zeta)+\eta^*(\zeta)} \operatorname{div} \ H\big(V^*(\rho), 0, \sigma^*, \pi^*\big) d\rho$$

$$\text{and} \quad N_r(\zeta) = \int_{-\infty}^\infty \phi_2^*(\eta)\frac{\partial H}{\partial r}\big(V^*(\eta), 0, \sigma^*, \pi^*\big) d\eta.$$

$N_r(\zeta)$ is independent of ζ for $r = \sigma, \pi$. We have

$$\phi_2(\eta; \zeta) = b(\zeta)B(\zeta)\phi_2^*(\eta)$$

and, for $r = \sigma, \pi$, or q,

$$\frac{\partial S_2}{\partial r}(\zeta, p^*) = \int_{-\infty}^\infty \psi_2(\xi; \zeta)\frac{\partial H}{\partial r}\Big(V^*\big(\xi + \eta^*(\zeta)\big), 0, \sigma^*, \pi^*\Big) d\xi$$

$$= \int_{-\infty}^\infty \phi_2(\eta; \zeta)\frac{\partial H}{\partial r}\big(V^*(\eta), 0, \sigma^*, \pi^*\big) d\eta = b(\zeta)B(\zeta)N_r(\zeta). \tag{8.18}$$

As in Proposition 8.4(7), we have

Proposition 8.6. *As $\xi \to -\infty$, all $\psi_{1j}^*(\xi)$ and $\phi_{2j}^*(\eta)$ go to 0 exponentially. As $\xi \to \infty$, $\psi_{11}^*(\xi)$ and $\phi_{23}^*(\eta)$ go to 0; $\psi_{12}^*(\xi)$, $\psi_{15}^*(\xi)$, $\phi_{24}^*(\eta)$ and $\phi_{25}^*(\eta)$ approach constants.*

8.5. Proofs of Proposition 8.1 and Corollary 8.2

We first prove Proposition 8.1.

Proof. From (8.6),

$$D(\zeta) = a(\zeta)b(\zeta)A(\zeta)B(\zeta)(M_\sigma N_\pi - M_\pi N_\sigma). \tag{8.19}$$

We need to show that $M_\sigma N_\pi - M_\pi N_\sigma \neq 0$. Recall that separation functions $\hat{S}_i(\sigma, \pi)$ for the individual layers were defined in Section 4. From (4.15) we see that for $r = \sigma, \pi$,

$$M_r = \frac{\partial \hat{S}_1}{\partial r}(\sigma^*, \pi^*) \quad \text{and} \quad N_r = \frac{\partial \hat{S}_2}{\partial r}(\sigma^*, \pi^*).$$

Since $\sigma_i(\pi)$ satisfies $\hat{S}_i(\sigma_i(\pi), \pi) = 0$, we have

$$\sigma_i'(\pi^*) = -\frac{\partial \hat{S}_i}{\partial \sigma}(\sigma^*, \pi^*) / \frac{\partial \hat{S}_i}{\partial \pi}(\sigma^*, \pi^*).$$

Since $(\sigma_1 - \sigma_2)'(\pi^*) \neq 0$,

$$M_\sigma N_\pi - M_\pi N_\sigma = \frac{\partial \hat{S}_1}{\partial \sigma}(\sigma^*, \pi^*)\frac{\partial \hat{S}_2}{\partial \pi}(\sigma^*, \pi^*) - \frac{\partial \hat{S}_1}{\partial \pi}(\sigma^*, \pi^*)\frac{\partial \hat{S}_2}{\partial \sigma}\sigma^*, \pi^*) \neq 0.$$

(8.20)

$\square$

Next we prove Corollary 8.2.

Proof. It is enough to show that $W^u(L_0)$ and $W^s(R_0)$ meet transversally within $\Sigma \times \sigma\pi$-space.

The intersection of $W^u(L_0)$ with $\Sigma \times \sigma\pi$-space is the image of the map

$$\mathcal{X}^u : \zeta_L \omega\sigma\pi\text{-space} \to X\sigma\pi\text{-space}$$

given by $\mathcal{X}^u(\zeta_L, \omega, \sigma, \pi) = \big(X^u(\zeta_L, \omega, \sigma, \pi), \sigma, \pi\big)$ Similarly, the intersection of $W^s(R_0)$ with $\Sigma \times \sigma\pi$-space is the image of the map

$$\mathcal{X}^s : \zeta_R \sigma\pi\text{-space} \to X\sigma\pi\text{-space}$$

given by $\mathcal{X}^s(\zeta_R, \sigma, \pi) = \big(X^s(\zeta_R, \sigma, \pi), \sigma, \pi\big)$. We have $\mathcal{X}^u(\zeta, 0, \sigma^*, \pi^*) = \mathcal{X}^s(\zeta, \sigma^*, \pi^*)$. We must show that the ranges of $D\mathcal{X}^u(\zeta, 0, \sigma^*, \pi^*)$ and $D\mathcal{X}^s(\zeta, \sigma^*, \pi^*)$ span the tangent space to $\Sigma \times \sigma\pi$-space at $\mathcal{X}^u(\zeta, 0, \sigma^*, \pi^*) = \mathcal{X}^s(\zeta, \sigma^*, \pi^*)$. Equivalently, define

$$\tilde{\mathcal{X}}^u : \zeta_L \omega\sigma\pi\text{-space} \to \zeta\gamma\delta\omega\sigma\pi\text{-space} \quad \text{and} \quad \tilde{\mathcal{X}}^s : \zeta_R\sigma\pi\text{-space} \to \zeta\gamma\delta\omega\sigma\pi\text{-space}$$

by

$$\tilde{\mathcal{X}}^u(\zeta_L, \omega, \sigma, \pi) = \big(\Phi \circ X^u(\zeta_L, \omega, \sigma, \pi), \sigma, \pi\big) \quad \text{and}$$
$$\tilde{\mathcal{X}}^s(\zeta_R, \sigma, \pi) = \big(\Phi \circ X^s(\zeta_R, \sigma, \pi), \sigma, \pi\big).$$

We must show that the ranges of $D\tilde{\mathcal{X}}^u(\zeta, 0, \sigma^*, \pi^*)$ and $D\tilde{\mathcal{X}}^s(\zeta, \sigma^*, \pi^*)$ span $\zeta\gamma\delta\omega\sigma\pi$-space. The sum of these ranges is the span of the column vectors in the following matrix:

$$
\begin{pmatrix}
1 & 0 & 0 & 0 & 0 & 0 \\
0 & \frac{\partial\gamma^u}{\partial\omega}(\zeta, p^*) & \frac{\partial\gamma^u}{\partial\sigma}(\zeta, p^*) & \frac{\partial\gamma^u}{\partial\pi}(\zeta, p^*) & \frac{\partial\gamma^\sigma}{\partial\sigma}(\zeta, p^*) & \frac{\partial\gamma^s}{\partial\pi}(\zeta, p^*) \\
0 & \frac{\partial\delta^u}{\partial\omega}(\zeta, p^*) & \frac{\partial\delta^u}{\partial\sigma}(\zeta, p^*) & \frac{\partial\delta^u}{\partial\pi}(\zeta, p^*) & \frac{\partial\delta^s}{\partial\sigma}(\zeta, p^*) & \frac{\partial\delta^s}{\partial\pi}(\zeta, p^*) \\
0 & 1 & 0 & 0 & 0 & 0 \\
0 & 0 & 1 & 0 & 1 & 0 \\
0 & 0 & 0 & 1 & 0 & 1
\end{pmatrix}.
$$

Equivalently, we may use the matrix

$$
\begin{pmatrix}
1 & 0 & 0 & 0 & 0 & 0 \\
0 & \frac{\partial\gamma^u}{\partial\omega}(\zeta, 0, p^*) & \frac{\partial\gamma^u}{\partial\sigma}(\zeta, 0, p^*) - \frac{\partial\gamma^s}{\partial\sigma}(\zeta, p^*) & \frac{\partial\gamma^u}{\partial\pi}(\zeta, 0, p^*) - \frac{\partial\gamma^s}{\partial\pi}(\zeta, p^*) & \frac{\partial\gamma^s}{\partial\sigma}(\zeta, p^*) & \frac{\partial\gamma^s}{\partial\pi}(\zeta, p^*) \\
0 & \frac{\partial\delta^u}{\partial\omega}(\zeta, 0, p^*) & \frac{\partial\delta^u}{\partial\sigma}(\zeta, 0, p^*) - \frac{\partial\delta^s}{\partial\sigma}(\zeta, p^*) & \frac{\partial\delta^u}{\partial\pi}(\zeta, 0, p^*) - \frac{\partial\delta^s}{\partial\sigma}(\zeta, p^*) & \frac{\partial\delta^s}{\partial\sigma}(\zeta, p^*) & \frac{\partial\delta^s}{\partial\pi}(\zeta, p^*) \\
0 & 1 & 0 & 0 & 0 & 0 \\
0 & 0 & 0 & 0 & 1 & 0 \\
0 & 0 & 0 & 0 & 0 & 1
\end{pmatrix}.
$$

This matrix has nonzero determinant if and only if

$$
\det\begin{pmatrix}
\frac{\partial\gamma^u}{\partial\sigma}(\zeta, 0, p^*) - \frac{\partial\gamma^s}{\partial\sigma}(\zeta, p^*) & \frac{\partial\gamma^u}{\partial\pi}(\zeta, 0, p^*) - \frac{\partial\gamma^s}{\partial\pi}(\zeta, p^*) \\
\frac{\partial\delta^u}{\partial\sigma}(\zeta, 0, p^*) - \frac{\partial\delta^s}{\partial\sigma}(\zeta, p^*) & \frac{\partial\delta^u}{\partial\pi}(\zeta, 0, p^*) - \frac{\partial\delta^s}{\partial\sigma}(\zeta, p^*)
\end{pmatrix} \neq 0.
$$

This is equivalent to $D(\zeta) \neq 0$. $\qquad\square$

8.6. Proof of Theorem 8.3

Proposition 8.7. (1) As $\zeta \to \alpha$, $\frac{\partial\pi}{\partial q}(\zeta, 0)$ grows like a constant plus

$$
-\frac{N_\sigma \psi_{15}^*(\infty) v_L^*}{M_\sigma N_\pi - M_\pi N\sigma} \eta^*(\zeta).
$$

(2) As $\zeta \to \beta$, $\frac{\partial\pi}{\partial q}(\zeta, 0)$ grows like a constant plus

$$
\frac{M_\sigma \phi_{25}^*(\infty) u_L^*}{M_\sigma N_\pi - M_\pi N\sigma} \eta^*(\zeta).
$$

Recall that $M_\sigma N_\pi - M_\pi N\sigma \neq 0$ by (8.20). From their definitions, $M_\sigma > 0$, $N_\sigma > 0$, $\psi_{15}^*(\infty) < 0$, and $\phi_{25}^*(\infty) > 0$. Since $\lim_{\zeta \to \alpha} \eta^*(\zeta) = -\infty$ and $\lim_{\zeta \to \beta} \eta^*(\zeta) = \infty$, we see that $\lim_{\zeta \to \alpha} \frac{\partial\pi}{\partial q}(\zeta, 0) = -\text{sgn}(M_\sigma N_\pi - M_\pi N\sigma)\infty$ and $\lim_{\zeta \to \beta} \frac{\partial\pi}{\partial q}(\zeta, 0) = \text{sgn}(M_\sigma N_\pi - M_\pi N\sigma)\infty$. Hence this proposition implies Theorem 8.3. The remainder of this section is devoted to its proof.

Differentiating (8.5) with respect to q and setting $q = 0$ yields

$$\begin{pmatrix} \frac{\partial S_1}{\partial \sigma}(\zeta, p^*) & \frac{\partial S_1}{\partial \pi}(\zeta, p^*) \\ \frac{\partial S_2}{\partial \sigma}(\zeta, p^*) & \frac{\partial S_2}{\partial \pi}(\zeta, p^*) \end{pmatrix} \begin{pmatrix} \frac{\partial \sigma}{\partial q}(\zeta, 0) \\ \frac{\partial \pi}{\partial q}(\zeta, 0) \end{pmatrix} + \begin{pmatrix} \frac{\partial S_1}{\partial q}(\zeta, p^*) \\ \frac{\partial S_2}{\partial q}(\zeta, p^*) \end{pmatrix} = \begin{pmatrix} 0 \\ 0 \end{pmatrix}. \quad (8.21)$$

Since $D(\zeta) \neq 0$, (8.21) yields

$$\begin{pmatrix} \frac{\partial \sigma}{\partial q}(\zeta, 0) \\ \frac{\partial \pi}{\partial q}(\zeta, 0) \end{pmatrix} = -D(\zeta)^{-1} \begin{pmatrix} \frac{\partial S_2}{\partial \pi}(\zeta, p^*) & -\frac{\partial S_1}{\partial \pi}(\zeta, p^*) \\ -\frac{\partial S_2}{\partial \sigma}(\zeta, p^*) & \frac{\partial S_1}{\partial \sigma}(\zeta, p^*) \end{pmatrix} \begin{pmatrix} \frac{\partial S_1}{\partial q}(\zeta, p^*) \\ \frac{\partial S_2}{\partial q}(\zeta, p^*) \end{pmatrix}. (8.22)$$

From (8.22), (8.19), (8.16), and (8.18),

$$\frac{\partial \pi}{\partial q}(\zeta, 0) = \frac{M_q(\zeta) N_\sigma - M_\sigma N_q(\zeta)}{M_\sigma N_\pi - M_\pi N\sigma}.$$

We have

$$M_q(\zeta) = \int_{-\infty}^{\infty} \psi_{15}^*(\xi) v^* (\xi + \eta^*(\zeta)) \, d\xi - \int_{-\infty}^{\infty} \psi_{15}^*(\xi) u^*(\xi) \, d\xi \quad (8.23)$$

and

$$N_q(\zeta) = \int_{-\infty}^{\infty} \phi_{25}^*(\eta) v^*(\eta) \, d\eta - \int_{-\infty}^{\infty} \phi_{25}^*(\eta) u^* (\eta - \eta^*(\zeta)) \, d\eta. \quad (8.24)$$

We first consider (8.23) as ζ approaches α and β. The second integral of (8.23) is a constant independent of ζ.

To study the first integral of (8.23) as $\zeta \to \beta$, rewrite it as

$$\int_{-\infty}^{0} \psi_{15}^*(\xi) v^* (\xi + \eta^*(\zeta)) \, d\xi + \int_{0}^{\infty} \psi_{15}^*(\xi) v^* (\xi + \eta^*(\zeta)) \, d\xi.$$

As $\zeta \to \beta$, $\eta^*(\zeta) \to \infty$, and both integrals go to 0.

To study the first integral of (8.23) as $\zeta \to \alpha$, let $\epsilon > 0$ and choose $\delta > 0$ so that if $|\psi_{15}^*(\xi) - \psi_{15}^*(\infty)| < \delta$ and $|v - v_L^*| < \delta$ then $|\psi_{15}^*(\xi) v - \psi_{15}^*(\infty) v_L^*| < \epsilon$. Choose ξ_1 such that for $\xi > \xi_1$, $|\psi_{15}^*(\xi) - \psi_{15}^*(\infty)| < \delta$, and choose ξ_2 such that for $\xi < \xi_2$, $|v(\xi) - v_L^*| < \delta$. For ζ near α, $\eta^*(\zeta)$ is near $-\infty$, so $\xi_1 < \xi_2 - \eta^*(\zeta)$. Hence we can write the first integral of (8.23) as

$$\int_{-\infty}^{\xi_1} \psi_{15}^*(\xi) v^* (\xi + \eta^*(\zeta)) \, d\xi + \int_{\xi_1}^{\xi_2 - \eta^*(\zeta)} \psi_{15}^*(\xi) v^* (\xi + \eta^*(\zeta)) \, d\xi$$

$$+ \int_{\xi_2 - \eta^*(\zeta)}^{\infty} \psi_{15}^*(\xi) v^* (\xi + \eta^*(\zeta)) \, d\xi.$$

The first of these integrals is bounded by $\int_{-\infty}^{\xi_1} \psi_{15}^*(\xi) v_L^* \, d\xi$. For the second, we have

$$\int_{\xi_1}^{\xi_2 - \eta^*(\zeta)} |\psi_{15}^*(\xi) v^*(\xi + \eta^*(\zeta)) - \psi_{15}^*(\infty) v_L^*| \, d\xi$$

$$< \int_{\xi_1}^{\xi_2 - \eta^*(\zeta)} \epsilon \, d\xi < \epsilon(\xi_2 - \eta^*(\zeta) - \xi_1),$$

so the second integral lies between $(\psi_{15}^*(\infty) v_L^* \pm \epsilon)(\xi_2 - \eta^*(\zeta) - \xi_1)$. The third can be rewritten as

$$\int_{\xi_2}^{\infty} \psi_{15}(\eta - \eta^*(\zeta); \zeta) v^*(\eta) \, d\xi,$$

which converges and is bounded uniformly in ζ since ψ_{15} is bounded. Thus, as $\zeta \to \alpha$, the first integral of (8.23) grows like a constant minus $\psi_{15}^*(\infty) v_L^* \eta^*(\zeta)$.

Next, we consider (8.24) as ζ approaches α and β. The first integral is a finite constant independent of ζ, and the second approaches zero as $\zeta \to \alpha$. To study the second integral as $\zeta \to \beta$, let $\epsilon > 0$ and choose $\delta > 0$ so that if $|\phi_{25}^*(\eta) - \phi_{25}^*(\infty)| < \delta$ and $|u - u_L^*| < \delta$ then $|\phi_{25}^*(\eta) v - \phi_{25}^*(\infty) u_L^*| < \epsilon$. Choose η_1 such that for $\eta > \eta_1$, $|\phi_{25}^*(\eta) - \phi_{25}^*(\infty)| < \delta$, and choose η_2 such that for $\xi < \xi_2$, $|u(\xi) - u_L^*| < \delta$. For ζ near β, we have $\eta_1 < \eta_2 + \eta^*(\zeta)$, so we can write the first integral of (8.23) as

$$\int_{-\infty}^{\eta_1} \phi_{25}^*(\eta) u^*(\eta - \eta^*(\zeta)) \, d\eta + \int_{\eta_1}^{\eta_2 + \eta^*(\zeta)} \phi_{25}^*(\eta) u^*(\eta - \eta^*(\zeta)) \, d\eta$$

$$+ \int_{\eta_2 + \eta^*(\zeta)}^{\infty} \phi_{25}^*(\eta) u^*(\eta - \eta^*(\zeta)) \, d\eta.$$

The first and third integrals are bounded, and the second lies between $(\phi_{25}^*(\infty) u_L^* \pm \epsilon)(\eta_2 + \eta^*(\zeta) - \eta_1)$. Thus, as $\zeta \to \alpha$, the first integral of (8.24) grows like a constant plus $\phi_{25}^*(\infty) u_L^* \eta^*(\zeta)$.

9. NUMERICAL RESULTS AND METHODS

In this section, we give some numerical results for the PDE (2.25)–(2.28) on a finite domain $0 < x < l$, $t > 0$, as well as some ODE simulations that show the traveling wave directly.

For physical parameters we use typical values from [12] and [15], including $E = 0.15 \times 73,500$ kJ/kmole, and $R = 8.3143$ kJ/kmole K. We shift and rescale the temperature so that 0 corresponds to the initial temperature of the porous medium T_0, which we also take to be the ignition temperature, and 1 corresponds to $T_0 + 773.15$.
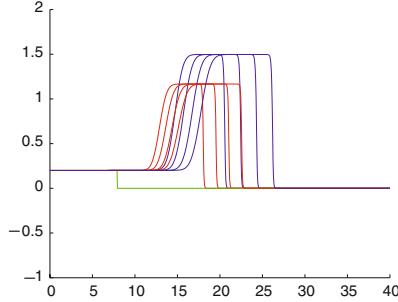
Figure 8. Temperature profiles in layers 1 and 2 at four equally spaced times $t_1 = 56.0$, $t_2 = 64.0$, $t_3 = 72.0$, and $t_4 = 80.0$, with $q = 0$.

For reference space, time, and temperature values we use $x^\star = 3.0$ m, $t^\star = 1.0$ D, and $T^\star = 773.15$ K, respectively. So, after dividing Eq. (2.25) by b_1 and (2.27) by b_2 we find the following dimensionless parameters: $a_1 = 19.4840$, $a_2 = 16.7032$, $b_1 = 1.0$, $b_2 = 1.0$, $c_1 = 1.8054$, $c_2 = 2.1063$, $d_1 = 62.5415$, $d_2 = 50.9796$, $A_1 = 5.4093$, $A_2 = 4.4093$, $\lambda_1 = 0.0815$, $\lambda_2 = 0.0815$. We use $l = 40$.

Let the PDE solution be $W(x, t) = \big(u(x, t), y(x, t), v(x, t), z(x, t)\big)$, $0 < x < l$. Our simulations use Neumann boundary conditions at $x = 0$ and $x = l$, and piecewise constant initial data

$$W(x, 0) = \begin{cases} (u_0, 0, v_0, 0), & \text{if } 0 < x < a, \\ (0, 1, 0, 1), & \text{if } a < x < l. \end{cases} \tag{9.1}$$

The values u_0 and v_0 can be interpreted as the gas injection temperatures at the left end $x = 0$ of layers 1 and 2, respectively. Note that at the start of the simulation, there is no fuel available for $0 < x < a$. For $a < x < 1$, all the fuel is available, and the temperature is 0. These initial conditions are appropriate for studying the propagation of a combustion front to the right.

Figure 8 shows a PDE simulation with $u_0 = v_0 = 0.2$ and $q = 0$. In each layer a traveling wave forms, but the waves have different left states (combustion temperature) and different speeds. The dimensionless combustion temperatures in layers 1 and 2 are approximately 1.15 and 1.50, respectively, and the wave speeds are approximately 0.18 and 0.24.

Figure 9 shows a PDE simulation with $u_0 = v_0 = 0.2$ and $q = 0.47$. Moving from right to left, we see that ahead of the combustion front the temperature is 0 (the initial temperature). In the combustion zones, which differ in the two layers, the temperature rises rapidly to the layer combustion temperature, which is higher in layer 1 than layer 2, as in
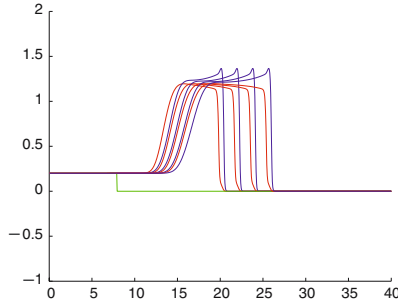
Figure 9. Temperature profiles in layers 1 and 2 at four equally spaced times $t_1 = 56.0$, $t_2 = 64.0$, $t_3 = 72.0$, and $t_4 = 80.0$, with $q = 0.47$.

Figure 8. Behind the combustion zones the temperatures slowly equilibrate at a high value, consistent with the analysis in Section 7. The part of the solution from here to the right propagates as a traveling wave. Behind this point the solution in each layer approaches the injection temperature. The dimensionless combustion temperatures in layers 1 and 2 are approximately 1.15 and 1.40, respectively, and the traveling wave speed is approximately 0.23.

For comparison, Figure 10 shows plots of the u-, v-, and w-coordinates of the strong heteroclinic solution of the ODEs (3.3)–(3.7) with $q = 0.47$, which occurs for $\sigma = 0.223076$. The solutions were computed on a time-interval of length 20, which in the plots is normalized to $0 \leqslant \tau \leqslant 1$. Note that the fast jump in u (respectively, v) occurs slightly before (respectively, after) $\tau = 0.70$. Before the jump, the u- and v- components change slowly from equal values (approximately 1.25) to different layer combustion temperatures. Meanwhile w is slowly increasing; it then jumps quickly to near 0. This picture is consistent with the analysis of the traveling wave for small q at the end of Section 7.
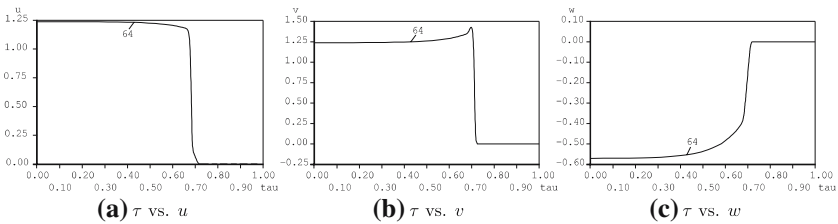

(a) τ vs. u **(b)** τ vs. v **(c)** τ vs. w

Figure 10. The u-, v-, and w-coordinates of the strong heteroclinic solution with $q = 0.47$ and $\sigma = 0.223076$.
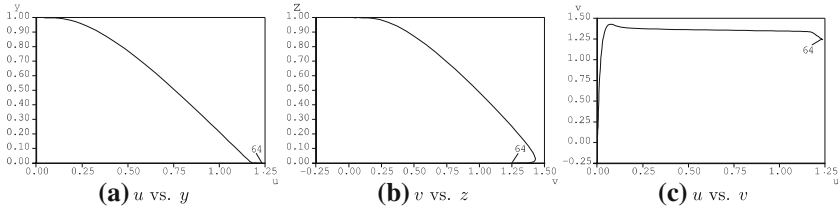
Figure 11. Three views of the strong heteroclinic orbit with $q = 0.47$, and $\sigma = 0.223076$.

Figure 11 shows three different projections of the same solution in phase space. The uy-plot includes an initial portion in which u slowly decreases from near 1.25 while y remains near 0; the vz-plot includes an initial portion in which v slowly increases from near 1.25 while z remains near 0. Recall from Section 7 that the slow manifold L_0 has $y = z = 0$. The uv plot shows the initial slow portion of the solution as a short diagonal at the right. After this slow portion, the solution jumps first in u, then in v.

Figure 12 shows a PDE simulation with $u_0 = v_0 = 0.2$ and $q = 117.61$. Temperature profiles in the two layers are extremely close, with dimensionless combustion temperature approximately 1.30 and wave speed approximately 0.21.

This is consistent with the analysis in Section 6, where solutions for large q are shown to lie near the manifold $u = v$. For comparison, Figure 13 shows plots of the u- and v-coordinates of the strong heteroclinic solution with $q = 117.61$ and $\sigma = 0.203274$, and the projection of the same solution in phase space to the uv-plane. The solutions were computed on a time-interval of length 2, which in the plots is normalized to $0 \leqslant \tau \leqslant 1$.
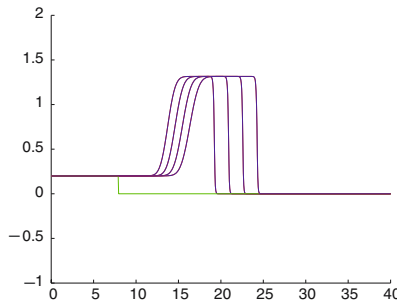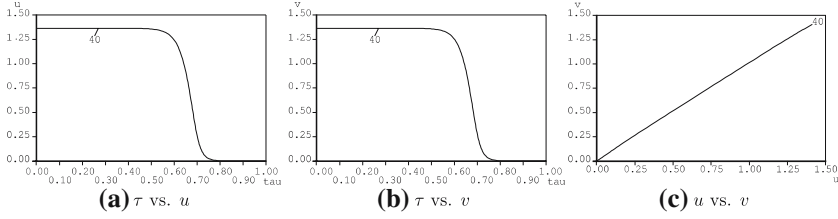

Figure 12. Temperature profiles in layers 1 and 2 at four equally spaced times $t_1 = 56.0$, $t_2 = 64.0$, $t_3 = 72.0$, and $t_4 = 80.0$, with $q = 117.61$.

(a) τ vs. u **(b)** τ vs. v **(c)** u vs. v

Figure 13. The u- and v-coordinates of the strong heteroclinic solution with $q = 117.61$ and $\sigma = 0.203274$, and the projection of the same solution in phase space to the uv-plane.

The PDE simulations in Figure 14 show that the traveling combustion wave that forms is independent of the injection temperature, provided the injection temperature is sufficiently large. It depends only on the system parameters and q, consistent with our analysis. The PDE simulation in Figure 15 shows that if the injection temperature is too small, no combustion wave forms.

To describe our numerical method for the PDEs (2.25)–(2.28), let $h = \Delta x = l/M$, $k = \Delta t = t_0/N$, $x_i = ih$, $t_n = nk$, where M and N denote the respective number of intervals in $[0, l]$ and $[0, t_0]$ for some $t_0 < \infty$. For each mesh point $(x_i, t_n) \in [0, L] \times [0, t_0]$ let $W_i^n = W(x_i, t_n)$, and let $W^n = W(x, t_n)$ when x_i does not need to be specified.

Suppose we know the solution $W^n = (u^n, y^n, v^n, z^n)$ at time t_n. Equations (2.26) and (2.28) are linear in y and z, respectively. Therefore, fixing $u = u^n$ and $v = v^n$, we can find y^{n+1} and z^{n+1} by solving these ODEs with initial conditions $y = y^n$ and $z = z^n$, respectively. We obtain

$$y^{n+1} = y^n \exp\left(-A_1 g(u^n)k\right) \quad \text{and} \quad z^{n+1} = z^n \exp\left(-A_2 g(v^n)k\right), \quad (9.2)$$
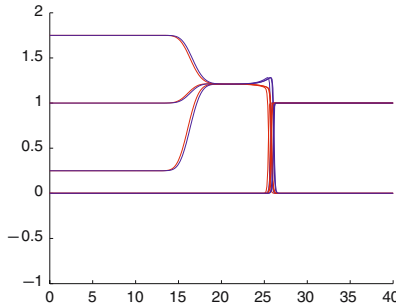
where $g(w) = \exp(-E/RT^*w)$.

Figure 14. Temperature and fuel consumption profiles for three different injection temperatures with $q = 1.18$.
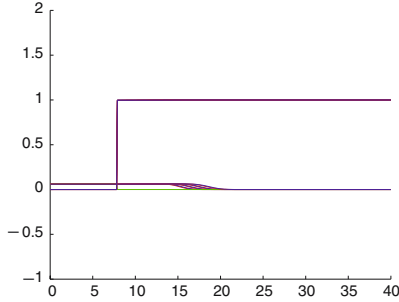
Figure 15. Temperature and fuel consumption profiles for low-injection temperatures with $q = 1.18$. A region of slightly elevated temperature propagates to the right, in which a very small amount of fuel has been consumed (only visible at greater magnification).

The other new values u^{n+1} and v^{n+1} are found after substituting y^{n+1} and z^{n+1} in (2.25) and (2.27) and solving the corresponding problem by some numerical method. We use the Crank–Nicholson implicit finite-difference scheme. Alternatively, we could have used finite-difference approximations associated with monotone iteration from a lower solution (see [14]).

The ODE strong heteroclinic solutions are computed using the boundary-value problem continuation routine of AUTO [8]. The boundary conditions state that at time T_1 (respectively, time T_2) the solution is in the linear approximation to the unstable manifold at X_L (respectively, the linear approximation to the stable manifold at X_R). Once such a solution is known for some value of the parameters, the parameters can be varied one at a time and the solution followed. The times $T_1 < T_2$ are also treated as parameters, so that the length of the time interval can be changed when necessary. An integral condition is used to fix the phase of the heteroclinic solution [10]. The accuracy of a related numerical method is analyzed in [17]. The procedure is initialized as follows: by visual inspection of numerical phase portraits for the one-layer ODE (4.1) and (4.2), we identify approximate parameter values $(a_1, b_1, c_1, d_1, A_1, \lambda_1, \sigma)$ for which a strong heteroclinic solution $(u(\xi), y(\xi))$ exists; u_L is then calculated from (4.4). We then set the remaining parameters $a_2 = a_1$, $b_2 = b_1$, etc. For these parameter values and any q, the five-dimensional ODEs (3.3)–(3.7) has the approximate heteroclinic solution $(u, y, v, z, w) = (u(\xi), y(\xi), u(\xi), y(\xi), 0)$. We initialize AUTO at this solution.

ACKNOWLEDGMENTS

REFERENCES

1. Akkutlu, Y., and Yortsos, Y. C. (2003). The dynamics of in-situ combustion fronts in porous media. *Combust. Flame*. **134,** 239–247.
2. Bose, A. (1995). Symmetric and antisymmetric pulses in parallel coupled nerve fibres. *SIAM J. Appl. Math.* **55,** 1650–1674.
3. Carr, J. (1981). Applications of Centre Manifold Theory. Appl. Math. Sci. **35**, Springer, Berlin.
4. Chow, S.-N., and Lin, X.-B. (1990). Bifurcation of a homoclinic orbit with a saddle-node equilibrium. *Diff. Integral Eq.* **3,** 435–466.
5. Crookston, R. B., and Culham, W. E. (1979). A numerical simulation model for thermal recovery processes. *Soc. Pet. Eng. J.* **19**, 37–58.
6. Da Mota, J. C., Dantas, W., and Marchesin, D. (1999). Traveling waves for combustion in porous media. *Int. Ser. Num. Math.* Birkhauser, **129,** 177–187.
7. Da Mota, J. C., Dantas, W., and Marchesin, D. (2002). Combustion fronts in porous media. *SIAM J. Appl. Math.* **62,** 2175–2198.
8. Doedel, E., and Kernévez, J. (1986). *AUTO: Software for Continuation Problems in Ordinary Differential Equations with Applications.* Technical Report, California Institute of Technology, 1986. (Available at http://indy.cs.concordia.ca/auto.).
9. Fenichel, N. (1979). Geometric singular perturbation theory for ordinary differential equations. *J. Diff. Eqs.* **31,** 53–98.
10. Friedman, M. J., and Doedel, E. (1991). Numerical computation and continuation of invariant manifolds connecting fixed points. *SIAM J. Numer. Anal.* **28,** 789–808.
11. Gasser, I., and Szmolyan, P. (1993). A geometric singular perturbation analysis of detonation and deflagration waves. *SIAM J. Math. Anal.* **24,** 968–986.
12. Gottfried, B. S. (1965). A mathematical model of thermal oil recovery in linear systems. *Soc. Pet. Eng. J.* 196–210.
13. Jones, C. K. R. T. (1995). Geometric singular perturbation theory. *Dynamical Systems (Montecatini Terme, 1994), Lecture Notes in Math.* Vol. 1609, Springer, Berlin, 44–118.
14. Pao, C. V. (1999). Numerical analysis of coupled systems of nonlinear parabolic equations. *SIAM J. Numer. Anal.* **36,** 393–416.
15. Prats, M. (1986). *Thermal recovery. Henry L. Doherty Series 7.* Society of Petroleum Engineers, Richardson, TX.
16. Schecter, S. (1987). The saddle-node separatrix-loop bifurcation. *SIAM J. Math. Anal.* **18,** 1142–1156.
17. Schecter, S. (1993). Numerical computation of saddle-node homoclinic bifurcation points. *SIAM J. Numer. Anal.* **30,** 1155–1178.
18. Schecter, S., and Marchesin, D. (2001). Geometric singular perturbation analysis of oxidation heat pulses for two-phase flow in porous media. *Bol. Soc. Bras. Mat.* **32,** 237–270.
19. Schecter, S., and Marchesin, D. (2003). Oxidation heat pulses in two-phase expansive flow in porous media. *ZAMP*, **54,** 48–83.
20. Schult, D. A., Matkowsky, B. J., Volpert, V. A., and Fernandez-pello, A. C. (1996). Forced forward smolder combustion. *Combust. Flame.* **104,** 1–26.